

12-8-2017

Fibrous Material Microstructure Design for Optimal Damping Performance

Yutong Xue

Purdue University, xue46@purdue.edu

J Stuart Bolton

Purdue University, bolton@purdue.edu

Follow this and additional works at: <http://docs.lib.purdue.edu/herrick>

Xue, Yutong and Bolton, J Stuart, "Fibrous Material Microstructure Design for Optimal Damping Performance" (2017). *Publications of the Ray W. Herrick Laboratories*. Paper 168.

<http://docs.lib.purdue.edu/herrick/168>

This document has been made available through Purdue e-Pubs, a service of the Purdue University Libraries. Please contact epubs@purdue.edu for additional information.

5th Symposium on the Acoustics of Poro-Elastic Materials (SAPEM)

December 6th – 8th, 2017

Le Mans, France

FIBROUS MATERIAL MICROSTRUCTURE DESIGN FOR OPTIMAL DAMPING PERFORMANCE

Yutong (Tony) Xue, J. Stuart Bolton

Ray W. Herrick Laboratories
Purdue University
West Lafayette, IN, USA

Presentation available at Herrick E-Pubs: <http://docs.lib.purdue.edu/herrick/>



Xue

eux

Je suis heureux d'être ici!

Je suis heureux d'être ici!



5th Symposium on the Acoustics of Poro-Elastic Materials (SAPEM)

December 6th – 8th, 2017

Le Mans, France

FIBROUS MATERIAL MICROSTRUCTURE DESIGN FOR OPTIMAL DAMPING PERFORMANCE

Yutong (Tony) Xue, J. Stuart Bolton

Ray W. Herrick Laboratories
Purdue University
West Lafayette, IN, USA

Presentation available at Herrick E-Pubs: <http://docs.lib.purdue.edu/herrick/>

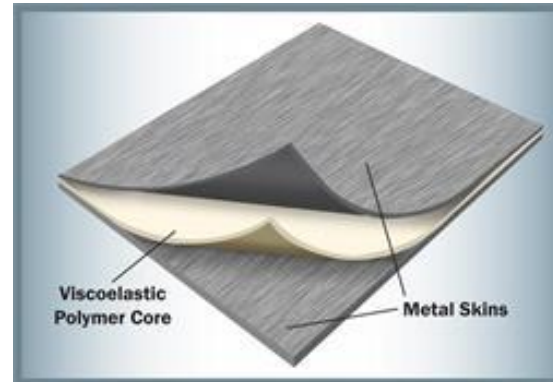


INTRODUCTION

- Traditional Damping Treatments – Visco-elastic Core with Metal Skins



Traditional Damping Material^[1]



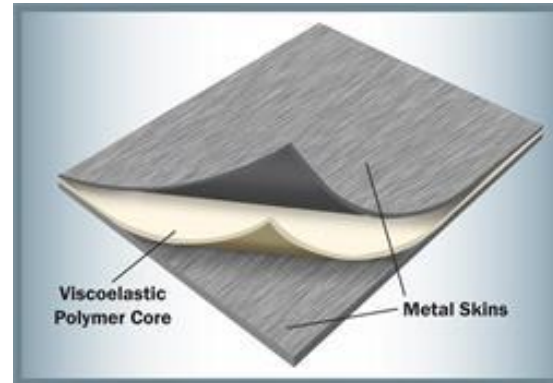
Structure of a Traditional Damper^[2]

INTRODUCTION

- **Traditional Damping Treatments – Visco-elastic Core with Metal Skins**



Traditional Damping Material^[1]



Structure of a Traditional Damper^[2]

- **Fibrous Damping Treatments – Target Material of this Study**



Fibrous Damping Material^[3]



Test on Fibrous Dampers^[4]

INTRODUCTION



- **Literature Review**

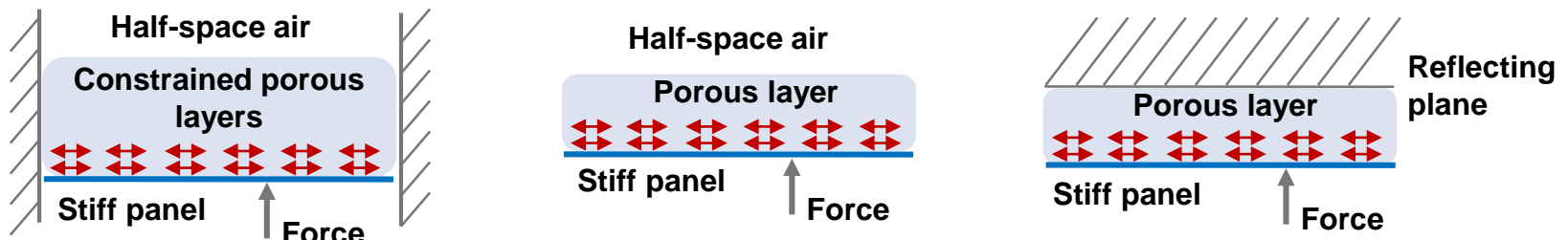
- **Bruer & Bolton, *AIAA 1987*^[5]** – Analysis of different waves propagating in the layered damping structures
- **Wahl & Bolton, *JASA 1992*^[6]** – Analysis by Inverse Discrete Fourier Transform (IDFT) on the spatial / temporal response of the layered damping system under line-driven force
- **Lai & Bolton, *Noise-Con 1998*^[7]** – Modeling to prove reasonable structural damping effect from the light fibrous materials through dissipating nearfield energy
- **Gerdes *et al.*, *Noise-Con 1998*^[8]** – Numerical modeling of the structural damping effect from the light fibrous materials by evaluating the in-plane direction particle velocity
- **S. Nadeau *et al.*, *Journal of Aircraft 1999*^[9]** – Tests of aircraft fuselage damping treatment by sound-absorbing blankets and related layered structures
- **Gerdes *et al.*, *Noise-Con 2001*^[4]** – Numerical modeling of the structural damping effect from three different visco-elastic dampers compared with fibrous dampers
- **Y. Xue and J. S. Bolton, *Inter-Noise 2017*^[10]** – Fibrous material airflow resistivity prediction based on accurate microstructure properties

INTRODUCTION

- **Literature Review**

- **Bruer & Bolton, *AIAA 1987*^[5]** – Analysis of different waves propagating in the layered damping structures
- **Wahl & Bolton, *JASA 1992*^[6]** – Analysis by Inverse Discrete Fourier Transform (IDFT) on the spatial / temporal response of the layered damping system under line-driven force
- **Lai & Bolton, *Noise-Con 1998*^[7]** – Modeling to prove reasonable structural damping effect from the light fibrous materials through dissipating nearfield energy
- **Gerdes *et al.*, *Noise-Con 1998*^[8]** – Numerical modeling of the structural damping effect from the light fibrous materials by evaluating the in-plane direction particle velocity
- **S. Nadeau *et al.*, *Journal of Aircraft 1999*^[9]** – Tests of aircraft fuselage damping treatment by sound-absorbing blankets and related layered structures
- **Gerdes *et al.*, *Noise-Con 2001*^[4]** – Numerical modeling of the structural damping effect from three different visco-elastic dampers compared with fibrous dampers
- **Y. Xue and J. S. Bolton, *Inter-Noise 2017*^[10]** – Fibrous material airflow resistivity prediction based on accurate microstructure properties

- **Layered Structures Shown in the Literature**



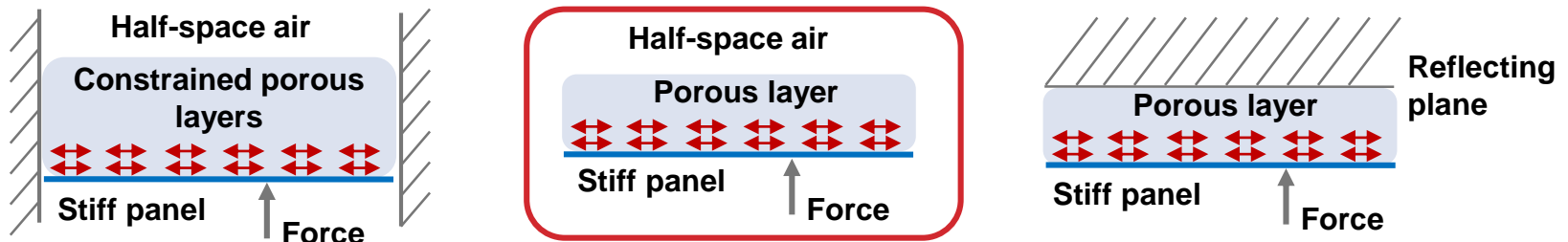
- The panel damping mostly arises because of the viscous interaction of the fibrous medium and the evanescent near-field of the panel associate with subsonic panel motion

INTRODUCTION

- Literature Review

- Bruer & Bolton, *AIAA 1987*^[5] – Analysis of different waves propagating in the layered damping structures
- Wahl & Bolton, *JASA 1992*^[6] – Analysis by Inverse Discrete Fourier Transform (IDFT) on the spatial / temporal response of the layered damping system under line-driven force
- Lai & Bolton, *Noise-Con 1998*^[7] – Modeling to prove reasonable structural damping effect from the light fibrous materials through dissipating nearfield energy
- Gerdes *et al.*, *Noise-Con 1998*^[8] – Numerical modeling of the structural damping effect from the light fibrous materials by evaluating the in-plane direction particle velocity
- S. Nadeau *et al.*, *Journal of Aircraft 1999*^[9] – Tests of aircraft fuselage damping treatment by sound-absorbing blankets and related layered structures
- Gerdes *et al.*, *Noise-Con 2001*^[4] – Numerical modeling of the structural damping effect from three different visco-elastic dampers compared with fibrous dampers
- Y. Xue and J. S. Bolton, *Inter-Noise 2017*^[10] – Fibrous material airflow resistivity prediction based on accurate microstructure properties

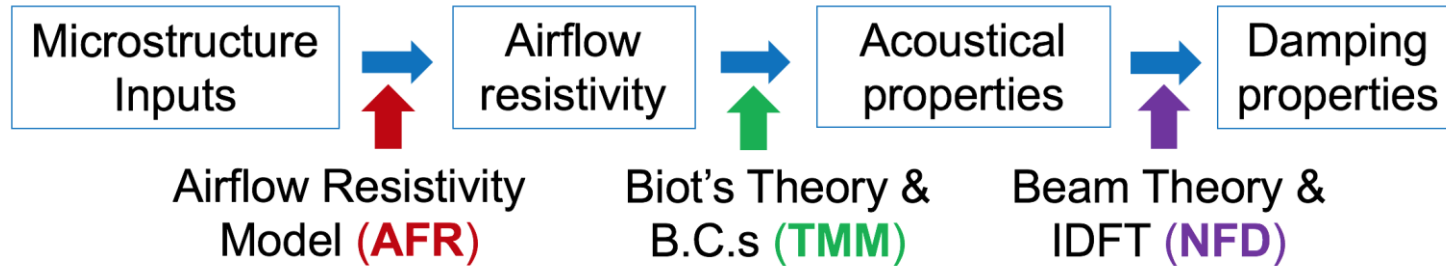
- Layered Structures Shown in the Literature



Target Structure of this Study

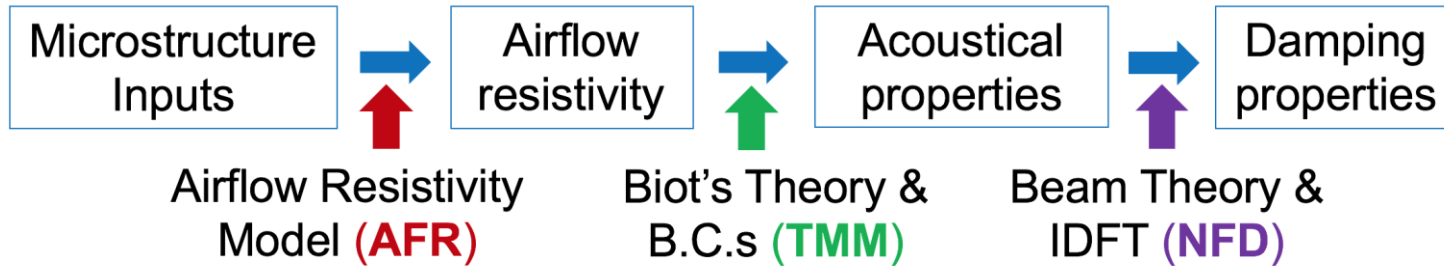
INTRODUCTION

- Acoustical / Damping Performance Prediction Process

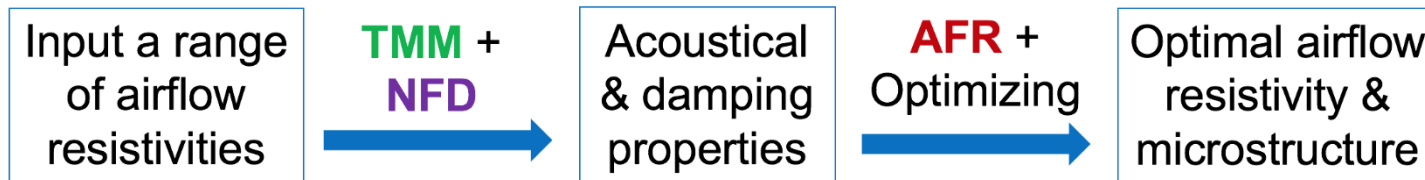


INTRODUCTION

- **Acoustical / Damping Performance Prediction Process**

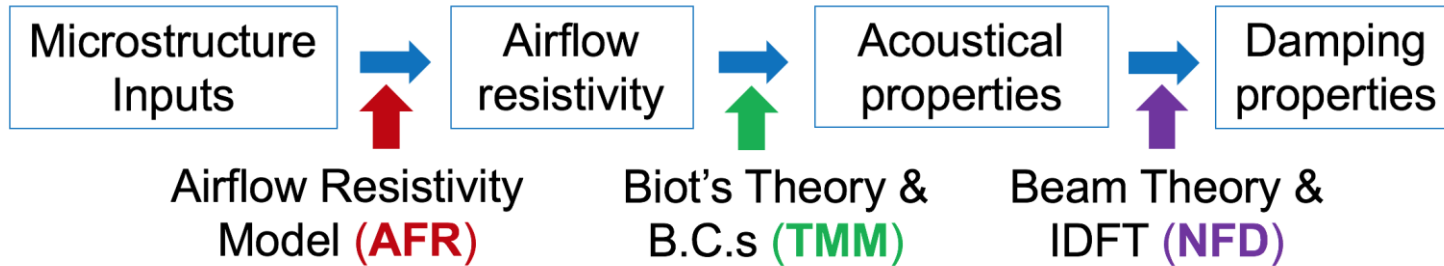


- **Noise Control Materials Microstructure Design Process**

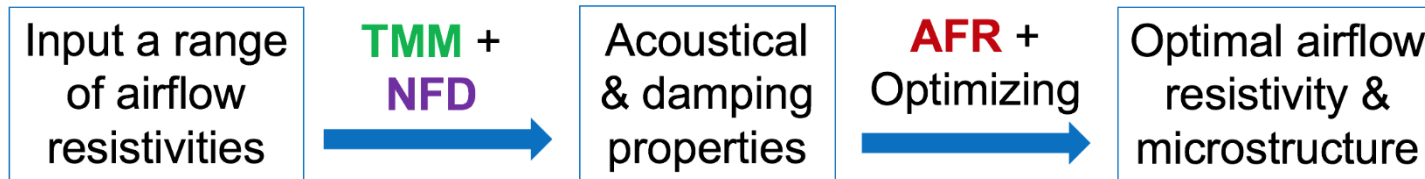


INTRODUCTION

- **Acoustical / Damping Performance Prediction Process**



- **Noise Control Materials Microstructure Design Process**



- **Objectives of this Study**

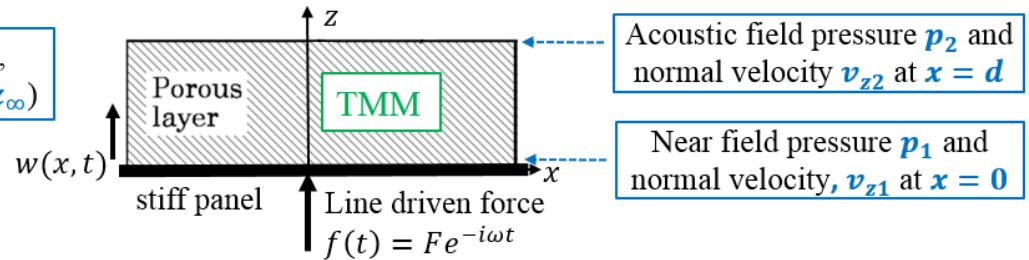
- Identify the airflow resistivity providing optimal damping performance given panel structure and frequency range of interest
- Translate the optimal airflow resistivity into optimal fiber sizes for fibrous material microstructure design

MODELING

- Modeling Process^{[6], [10]}

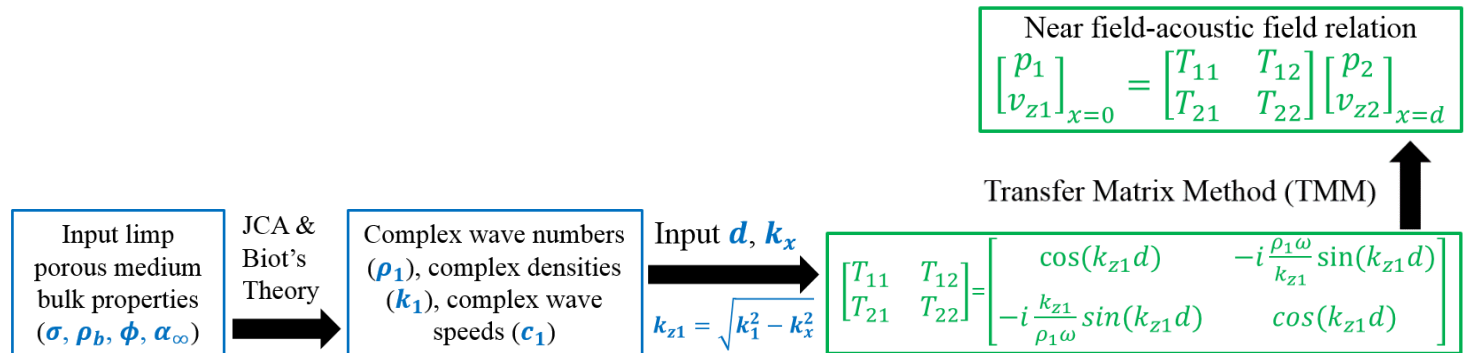
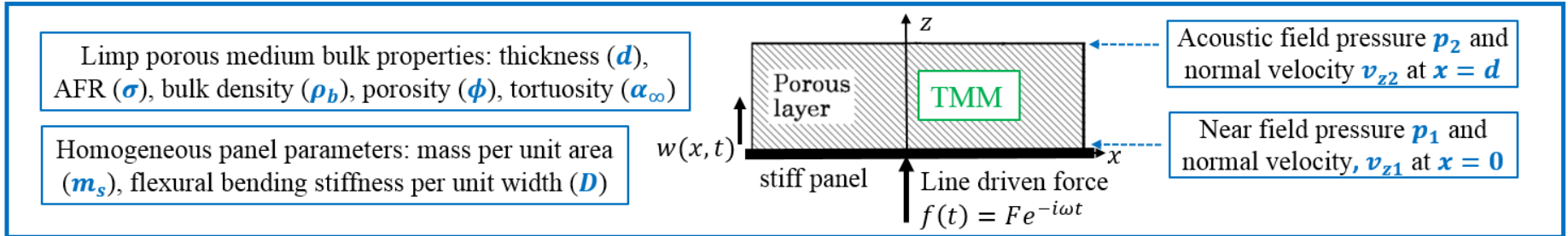
Limp porous medium bulk properties: thickness (d), AFR (σ), bulk density (ρ_b), porosity (ϕ), tortuosity (α_∞)

Homogeneous panel parameters: mass per unit area (m_s), flexural bending stiffness per unit width (D)



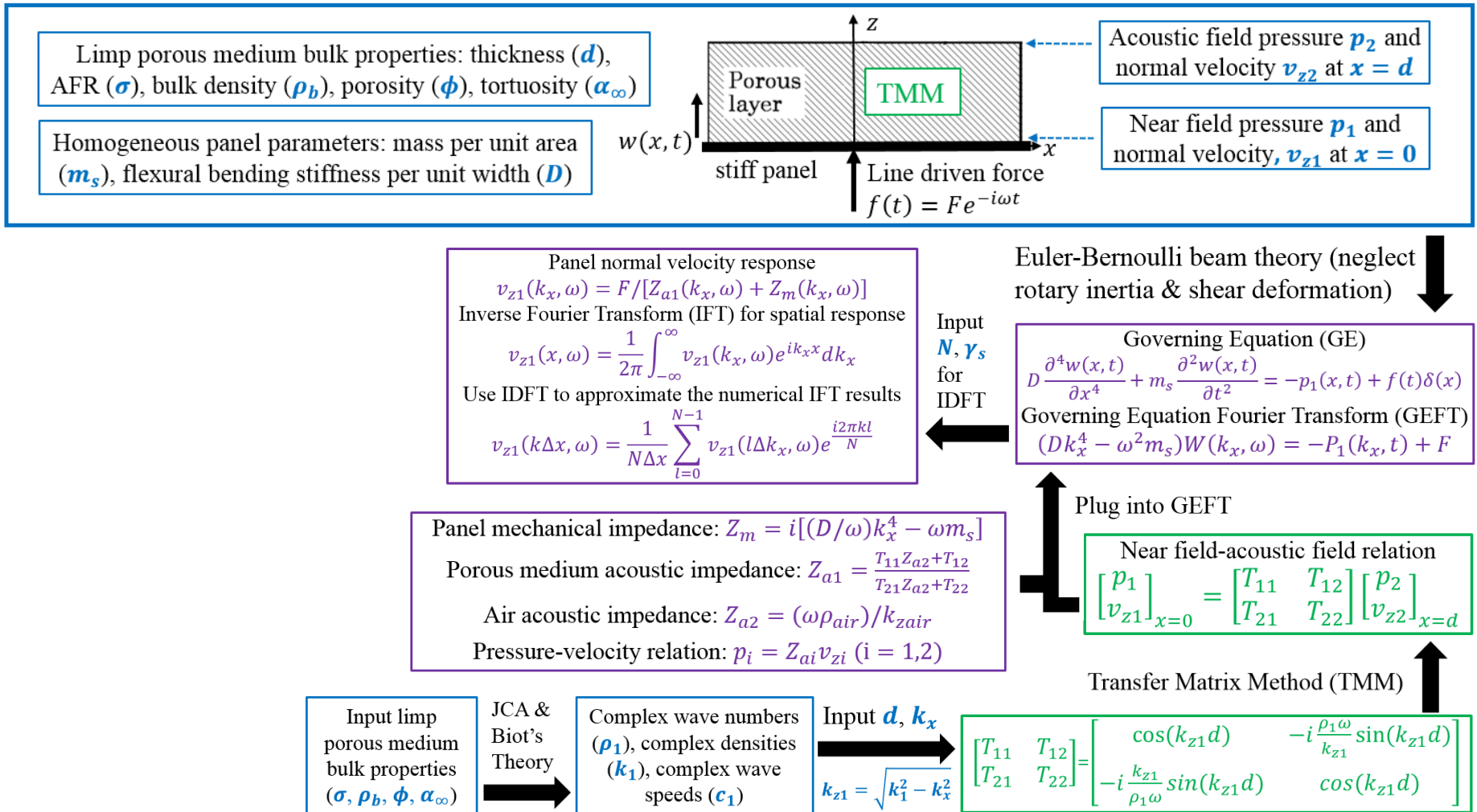
MODELING

- Modeling Process^{[6], [10]}



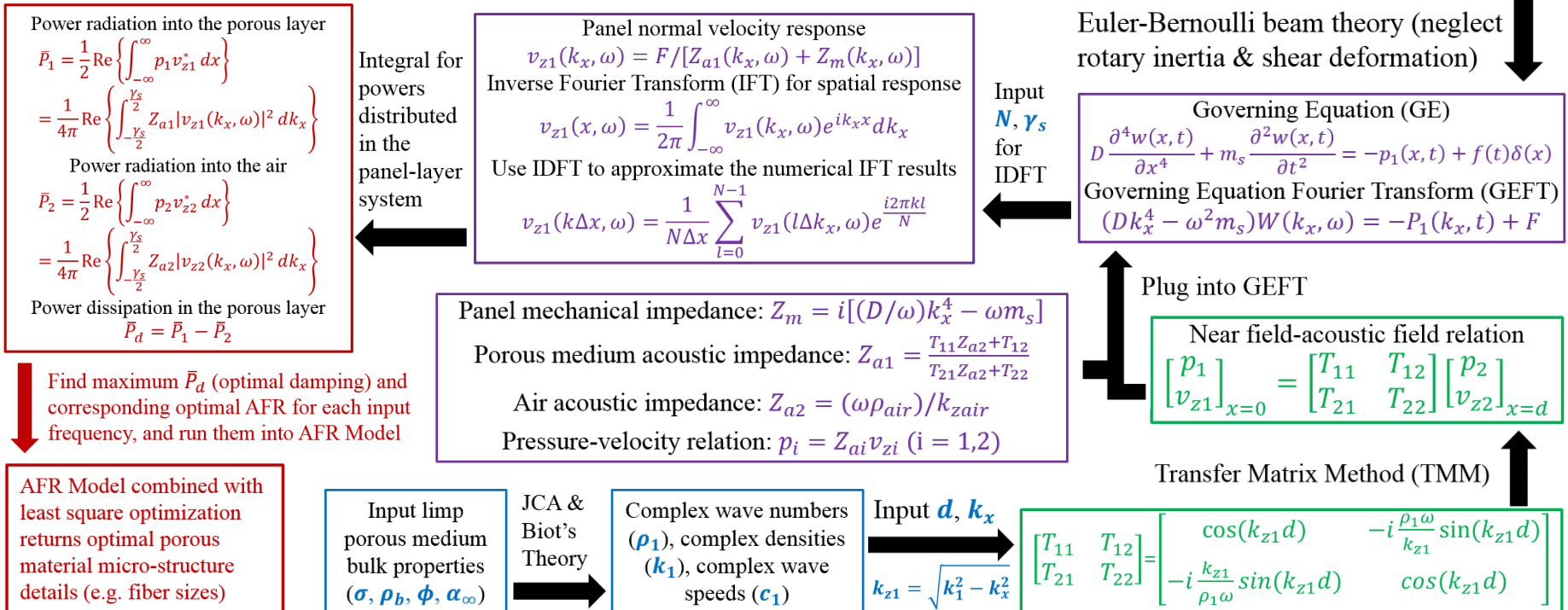
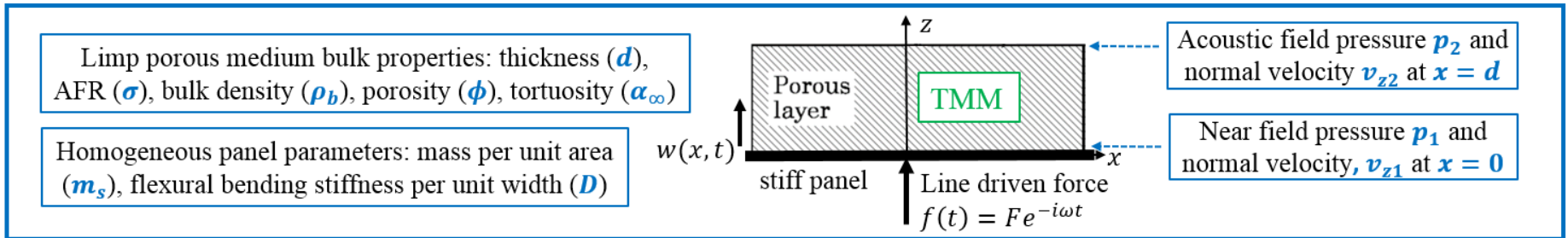
MODELING

- Modeling Process[6], [10]



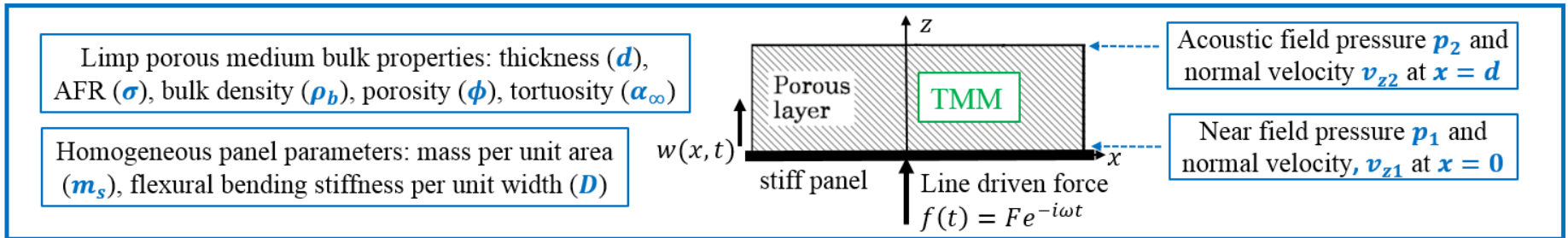
MODELING

- Modeling Process[6], [10]



MODELING

- Modeling Process[6], [10]



Power radiation into the porous layer

$$\bar{P}_1 = \frac{1}{2} \text{Re} \left\{ \int_{-\infty}^{\infty} p_1 v_{z1}^* dx \right\}$$

$$= \frac{1}{4\pi} \text{Re} \left\{ \int_{-\gamma_s/2}^{\gamma_s/2} Z_{a1} |v_{z1}(k_x, \omega)|^2 dk_x \right\}$$

Power radiation into the air

$$\bar{P}_2 = \frac{1}{2} \text{Re} \left\{ \int_{-\infty}^{\infty} p_2 v_{z2}^* dx \right\}$$

$$= \frac{1}{4\pi} \text{Re} \left\{ \int_{-\gamma_s/2}^{\gamma_s/2} Z_{a2} |v_{z2}(k_x, \omega)|^2 dk_x \right\}$$

Power dissipation in the porous layer

$$\bar{P}_d = \bar{P}_1 - \bar{P}_2$$

Integral for powers distributed in the panel-layer system

Panel normal velocity response

$$v_{z1}(k_x, \omega) = F / [Z_{a1}(k_x, \omega) + Z_m(k_x, \omega)]$$

Inverse Fourier Transform (IFT) for spatial response

$$v_{z1}(x, \omega) = \frac{1}{2\pi} \int_{-\infty}^{\infty} v_{z1}(k_x, \omega) e^{ik_x x} dk_x$$

Use IDFT to approximate the numerical IFT results

$$v_{z1}(k\Delta x, \omega) = \frac{1}{N\Delta x} \sum_{l=0}^{N-1} v_{z1}(l\Delta k_x, \omega) e^{i2\pi kl/N}$$

Input N, γ_s for IDFT

Euler-Bernoulli beam theory (neglect rotary inertia & shear deformation)

Governing Equation (GE)

$$D \frac{\partial^4 w(x, t)}{\partial x^4} + m_s \frac{\partial^2 w(x, t)}{\partial t^2} = -p_1(x, t) + f(t)\delta(x)$$

Governing Equation Fourier Transform (GEFT)

$$(Dk_x^4 - v\omega^2 m_s)W(k_x, \omega) = -P_1(k_x, \omega) + F$$

Plug into GEFT

Near field-acoustic field relation

$$\begin{bmatrix} p_1 \\ v_{z1} \end{bmatrix}_{x=0} = \begin{bmatrix} T_{11} & T_{12} \\ T_{21} & T_{22} \end{bmatrix} \begin{bmatrix} p_2 \\ v_{z2} \end{bmatrix}_{x=d}$$

Transfer Matrix Method (TMM)

Panel mechanical impedance: $Z_m = i[(D/\omega)k_x^4 - \omega m_s]$

Porous medium acoustic impedance: $Z_{a1} = \frac{T_{11}Z_{a2} + T_{12}}{T_{21}Z_{a2} + T_{22}}$

Air acoustic impedance: $Z_{a2} = (\omega\rho_{air})/k_{zair}$

Pressure-velocity relation: $p_i = Z_{ai}v_{zi} (i = 1, 2)$

$$\begin{bmatrix} T_{11} & T_{12} \\ T_{21} & T_{22} \end{bmatrix} = \begin{bmatrix} \cos(k_{z1}d) & -i\frac{\rho_1\omega}{k_{z1}} \sin(k_{z1}d) \\ -i\frac{k_{z1}}{\rho_1\omega} \sin(k_{z1}d) & \cos(k_{z1}d) \end{bmatrix}$$

Find maximum \bar{P}_d (optimal damping) and corresponding optimal AFR for each input frequency, and run them into AFR Model

AFR Model combined with least square optimization returns optimal porous material micro-structure details (e.g. fiber sizes)

Input limp porous medium bulk properties ($\sigma, \rho_b, \phi, \alpha_\infty$)

JCA & Biot's Theory

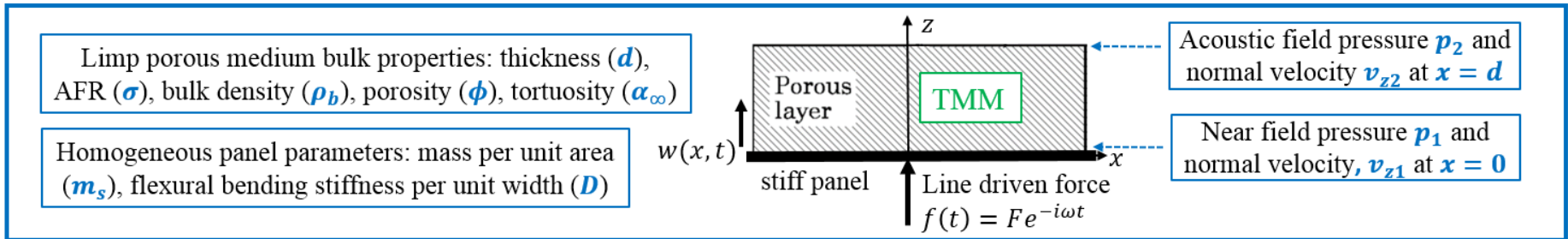
Complex wave numbers (ρ_1), complex densities (k_1), complex wave speeds (c_1)

Input d, k_x

$$k_{z1} = \sqrt{k_1^2 - k_x^2}$$

MODELING

- Modeling Process[6], [10]



Limp porous medium bulk properties: thickness (d), AFR (σ), bulk density (ρ_b), porosity (ϕ), tortuosity (α_∞)

Homogeneous panel parameters: mass per unit area (m_s), flexural bending stiffness per unit width (D)

Acoustic field pressure p_2 and normal velocity v_{z2} at $x = d$

Near field pressure p_1 and normal velocity, v_{z1} at $x = 0$

Power radiation into the porous layer

$$\bar{P}_1 = \frac{1}{2} \text{Re} \left\{ \int_{-\infty}^{\infty} p_1 v_{z1}^* dx \right\}$$

$$= \frac{1}{4\pi} \text{Re} \left\{ \int_{-\frac{Y_s}{2}}^{\frac{Y_s}{2}} Z_{a1} |v_{z1}(k_x, \omega)|^2 dk_x \right\}$$

Power radiation into the air

$$\bar{P}_2 = \frac{1}{2} \text{Re} \left\{ \int_{-\infty}^{\infty} p_2 v_{z2}^* dx \right\}$$

$$= \frac{1}{4\pi} \text{Re} \left\{ \int_{-\frac{Y_s}{2}}^{\frac{Y_s}{2}} Z_{a2} |v_{z2}(k_x, \omega)|^2 dk_x \right\}$$

Power dissipation in the porous layer

$$\bar{P}_d = \bar{P}_1 - \bar{P}_2$$

Integral for powers distributed in the panel-layer system

Panel normal velocity response

$$v_{z1}(k_x, \omega) = F / [Z_{a1}(k_x, \omega) + Z_m(k_x, \omega)]$$

Inverse Fourier Transform (IFT) for spatial response

$$v_{z1}(x, \omega) = \frac{1}{2\pi} \int_{-\infty}^{\infty} v_{z1}(k_x, \omega) e^{ik_x x} dk_x$$

Use IDFT to approximate the numerical IFT results

$$v_{z1}(k\Delta x, \omega) = \frac{1}{N\Delta x} \sum_{l=0}^{N-1} v_{z1}(l\Delta k_x, \omega) e^{\frac{i2\pi kl}{N}}$$

Input N, γ_s for IDFT

Euler-Bernoulli beam theory (neglect rotary inertia & shear deformation)

Governing Equation (GE)

$$D \frac{\partial^4 w(x, t)}{\partial x^4} + m_s \frac{\partial^2 w(x, t)}{\partial t^2} = -p_1(x, t) + f(t)\delta(x)$$

Governing Equation Fourier Transform (GEFT)

$$(Dk_x^4 - \omega^2 m_s)W(k_x, \omega) = -P_1(k_x, \omega) + F$$

Plug into GEFT

Near field-acoustic field relation

$$\begin{bmatrix} p_1 \\ v_{z1} \end{bmatrix}_{x=0} = \begin{bmatrix} T_{11} & T_{12} \\ T_{21} & T_{22} \end{bmatrix} \begin{bmatrix} p_2 \\ v_{z2} \end{bmatrix}_{x=d}$$

Panel mechanical impedance: $Z_m = i[(D/\omega)k_x^4 - \omega m_s]$

Porous medium acoustic impedance: $Z_{a1} = \frac{T_{11}Z_{a2} + T_{12}}{T_{21}Z_{a2} + T_{22}}$

Air acoustic impedance: $Z_{a2} = (\omega \rho_{air})/k_{zair}$

Pressure-velocity relation: $p_i = Z_{ai}v_{zi} (i = 1, 2)$

Transfer Matrix Method (TMM)

$$\begin{bmatrix} T_{11} & T_{12} \\ T_{21} & T_{22} \end{bmatrix} = \begin{bmatrix} \cos(k_{z1}d) & -i \frac{\rho_1 \omega}{k_{z1}} \sin(k_{z1}d) \\ -i \frac{k_{z1}}{\rho_1 \omega} \sin(k_{z1}d) & \cos(k_{z1}d) \end{bmatrix}$$

Find maximum \bar{P}_d (optimal damping) and corresponding optimal AFR for each input frequency, and run them into AFR Model

AFR Model combined with least square optimization returns optimal porous material micro-structure details (e.g. fiber sizes)

Input limp porous medium bulk properties ($\sigma, \rho_b, \phi, \alpha_\infty$)

JCA & Biot's Theory

Complex wave numbers (ρ_1), complex densities (k_1), complex wave speeds (c_1)

Input d, k_x
 $k_{z1} = \sqrt{k_1^2 - k_x^2}$

MODELING – KEY POINT 1

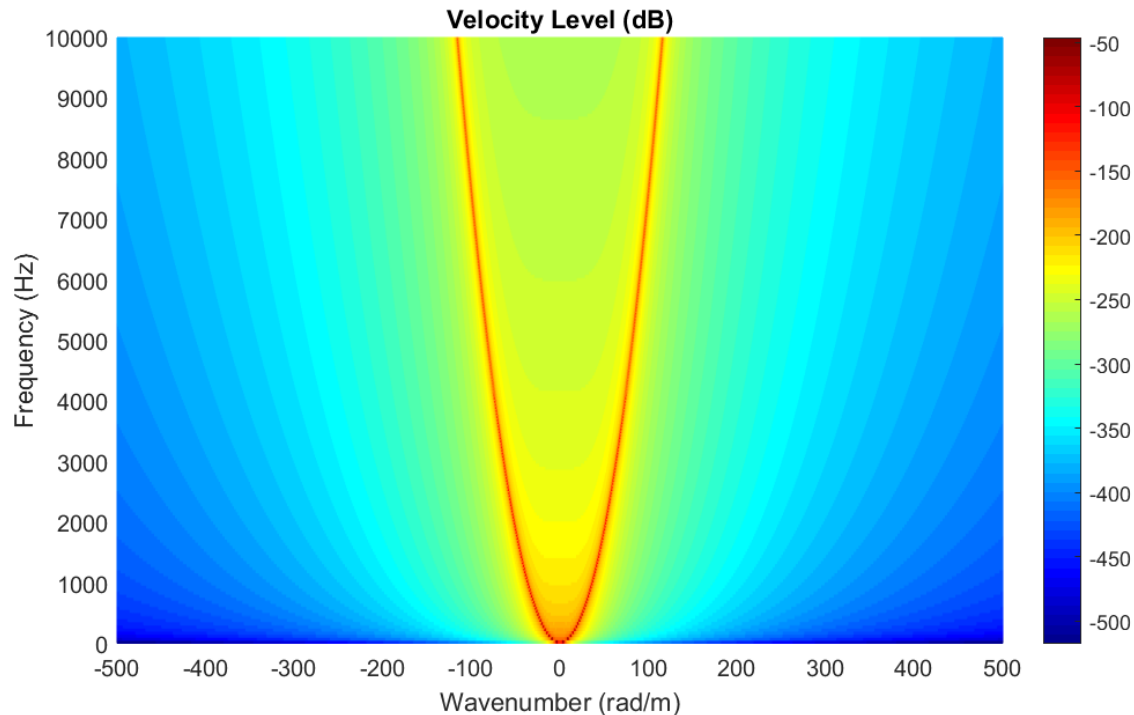


- Choice of IDFT sampling rate γ_s and sampling points number N

- **Target of the NFD model:** calculate spatial responses for wide frequency range
- **Key point:** for each frequency input, choosing proper γ_s and N to ensure **accurate IDFT results over a large enough spatial span** for observation

MODELING – KEY POINT 1

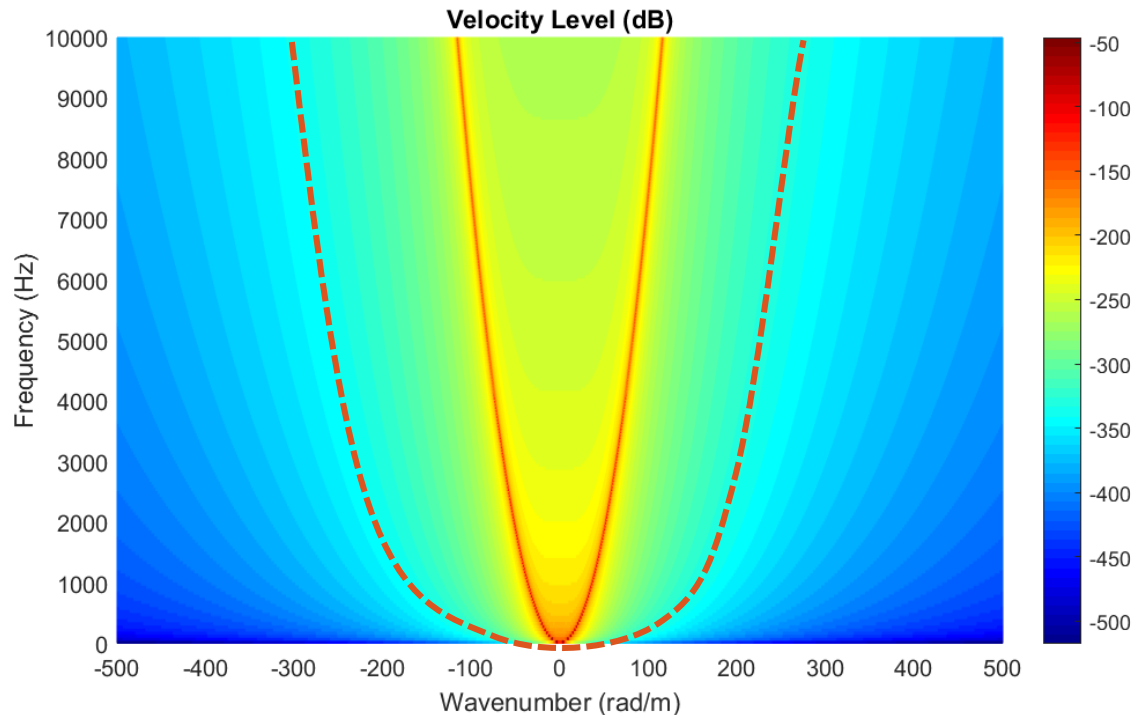
- Choice of IDFT sampling rate γ_s and sampling points number N
- **Target of the NFD model:** calculate spatial responses for wide frequency range
- **Key point:** for each frequency input, choosing proper γ_s and N to ensure **accurate IDFT results over a large enough spatial span** for observation



- Step 1: evaluate the wave number domain response of the panel

MODELING – KEY POINT 1

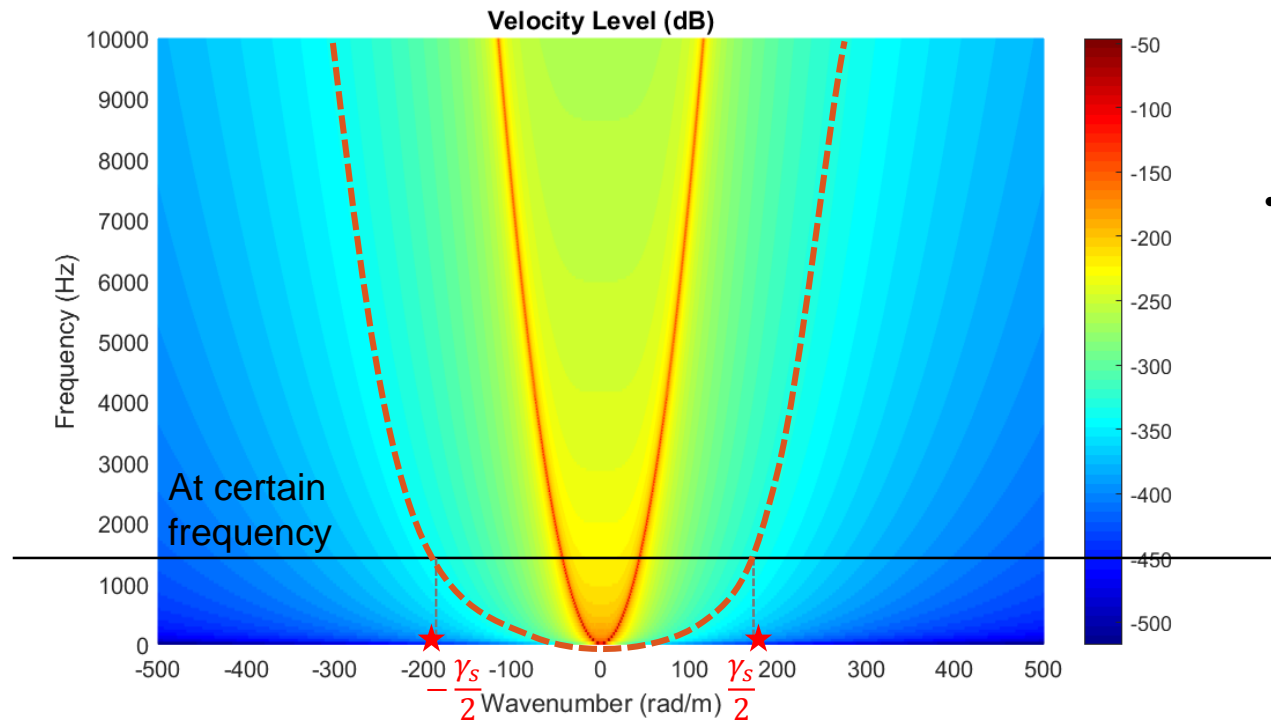
- Choice of IDFT sampling rate γ_s and sampling points number N
- **Target of the NFD model:** calculate spatial responses for wide frequency range
- **Key point:** for each frequency input, choosing proper γ_s and N to ensure **accurate IDFT results over a large enough spatial span** for observation



- Step 2: decide a proper cutoff level to avoid windowing/truncation effect

MODELING – KEY POINT 1

- Choice of IDFT sampling rate γ_s and sampling points number N
- **Target of the NFD model:** calculate spatial responses for wide frequency range
- **Key point:** for each frequency input, choosing proper γ_s and N to ensure **accurate IDFT results over a large enough spatial span** for observation

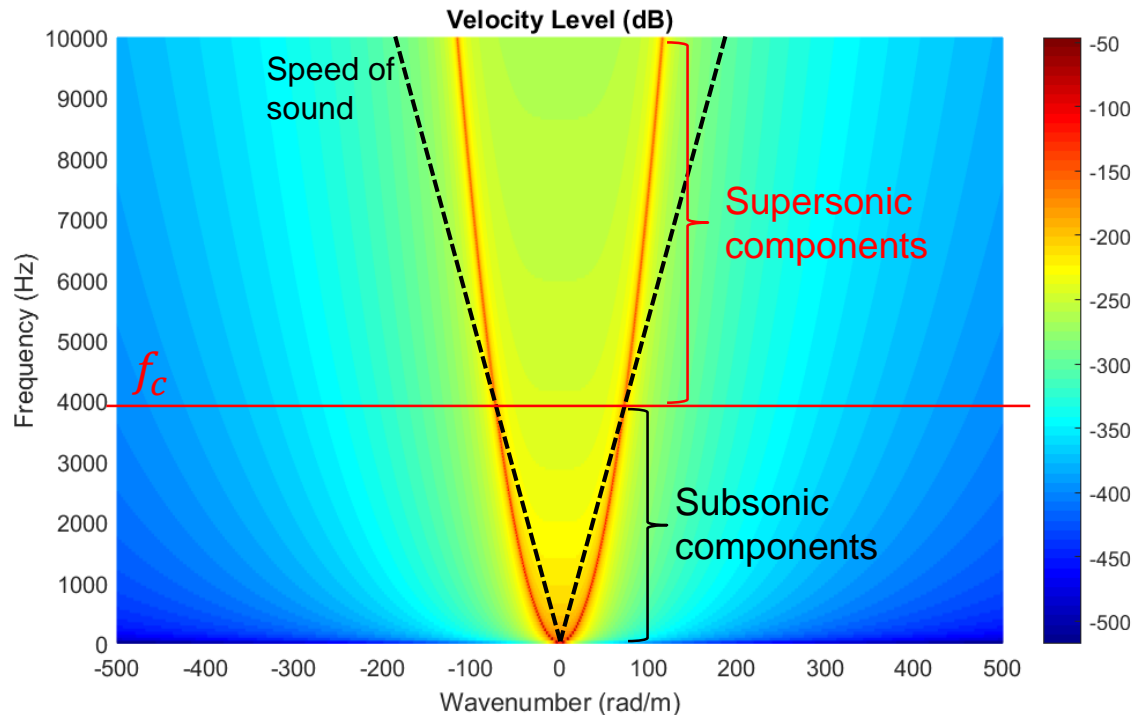


- N should be large enough to avoid bias

- Step 3: find the proper sampling rate γ_s for each input frequency

MODELING – KEY POINT 1

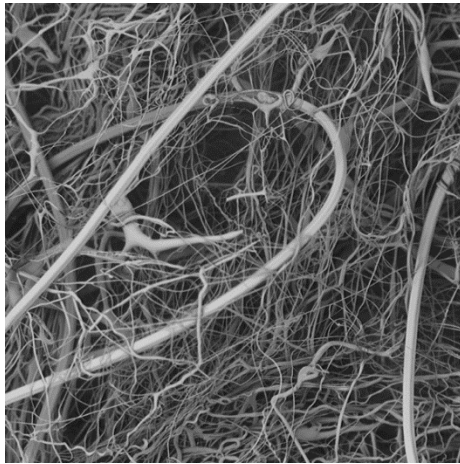
- Choice of IDFT sampling rate γ_s and sampling points number N
- **Target of the NFD model:** calculate spatial responses for wide frequency range
- **Key point:** for each frequency input, choosing proper γ_s and N to ensure **accurate IDFT results over a large enough spatial span** for observation



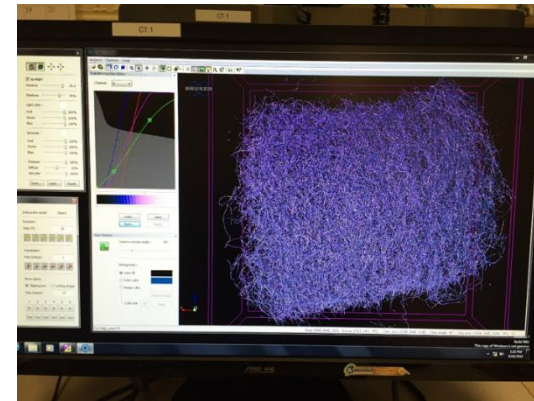
- Step 4: identify the critical frequency f_c

MODELING - KEY POINT 2

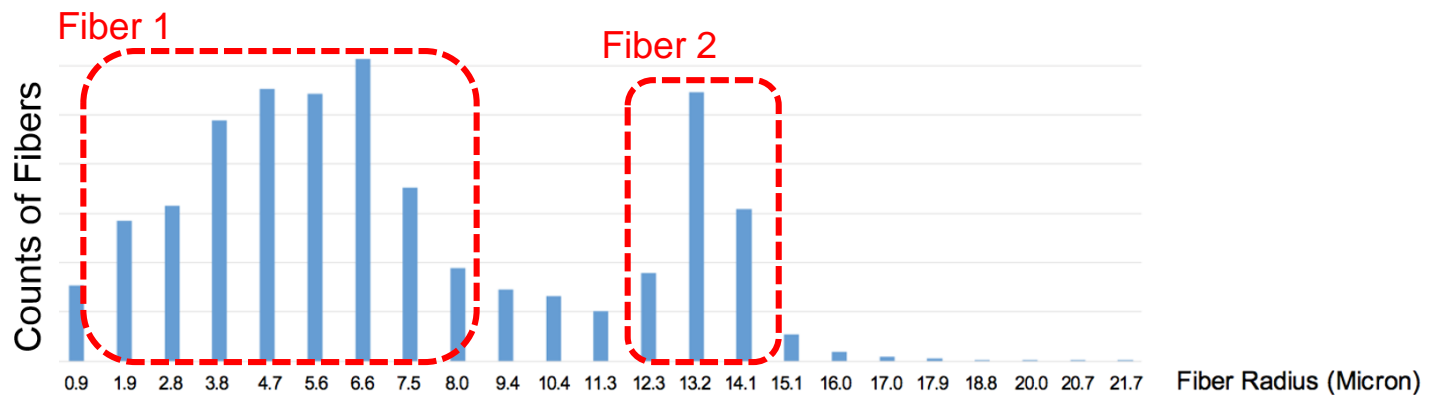
- Fibrous Medium Airflow Resistivity Prediction^[7]



SEM of the target fibrous medium



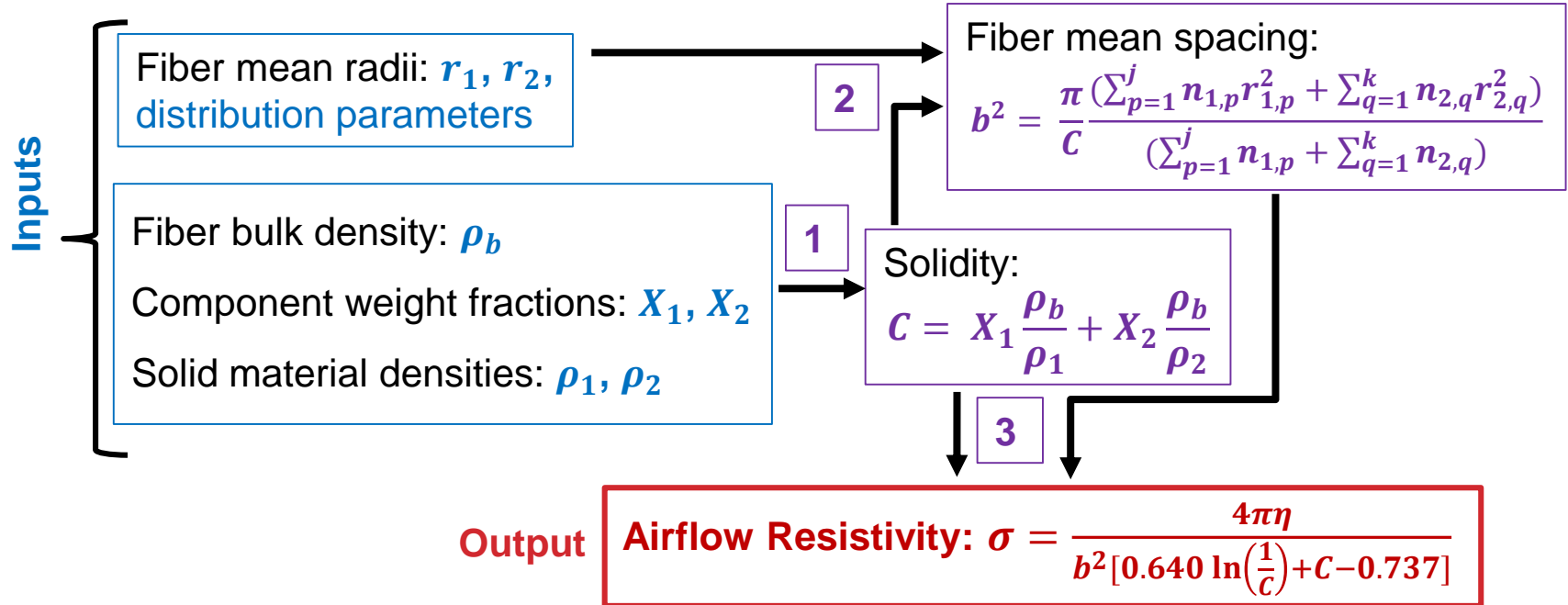
Fibrous medium micro-CT scanning



Micro-CT scanned fiber radii distribution of the fibrous medium

MODELING - KEY POINT 2

Fibrous Medium Airflow Resistivity Prediction^[7]



- **Step 1:** C calculation based on $\rho_b, X_1, X_2, \rho_1, \rho_2$
- **Step 2:** b^2 calculation based on r_1, r_2 , distribution parameters and C
- **Step 3:** σ calculation base on C and b^2

MODELING – KEY POINT 2



- Fibrous Medium Airflow Resistivity Prediction^[7]

Inputs

Fibrous medium verified
microstructure inputs

AFR



Output

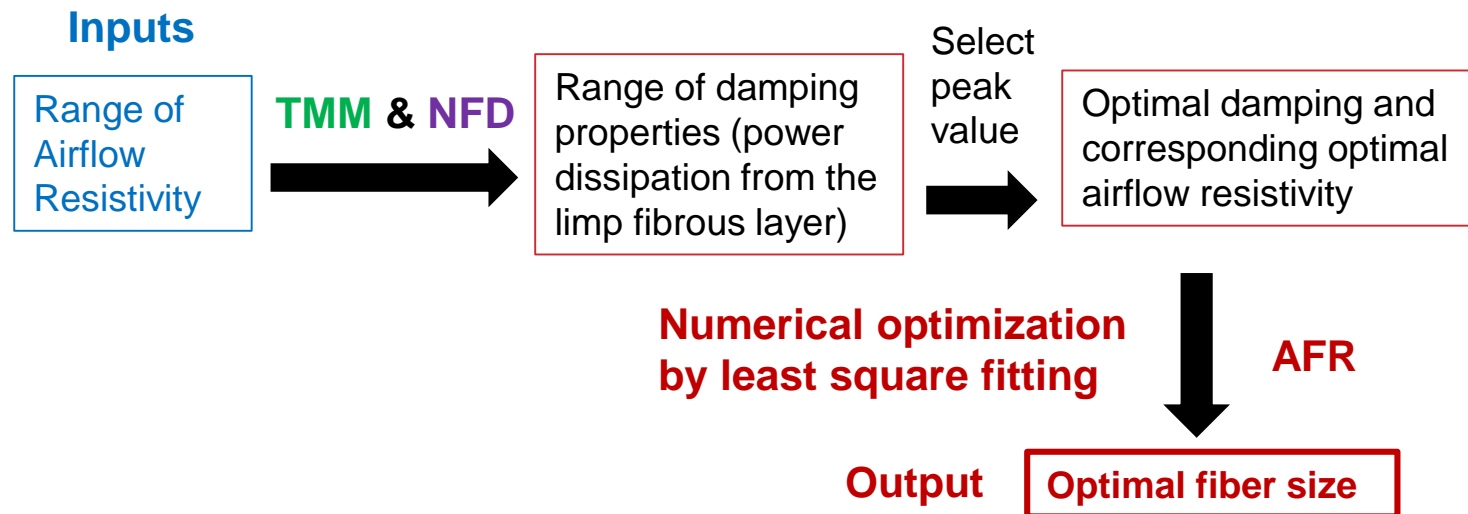
Airflow Resistivity Prediction

MODELING - KEY POINT 2

- Fibrous Medium Airflow Resistivity Prediction^[7]

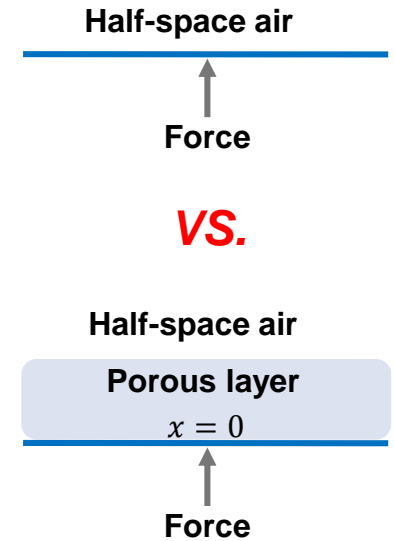
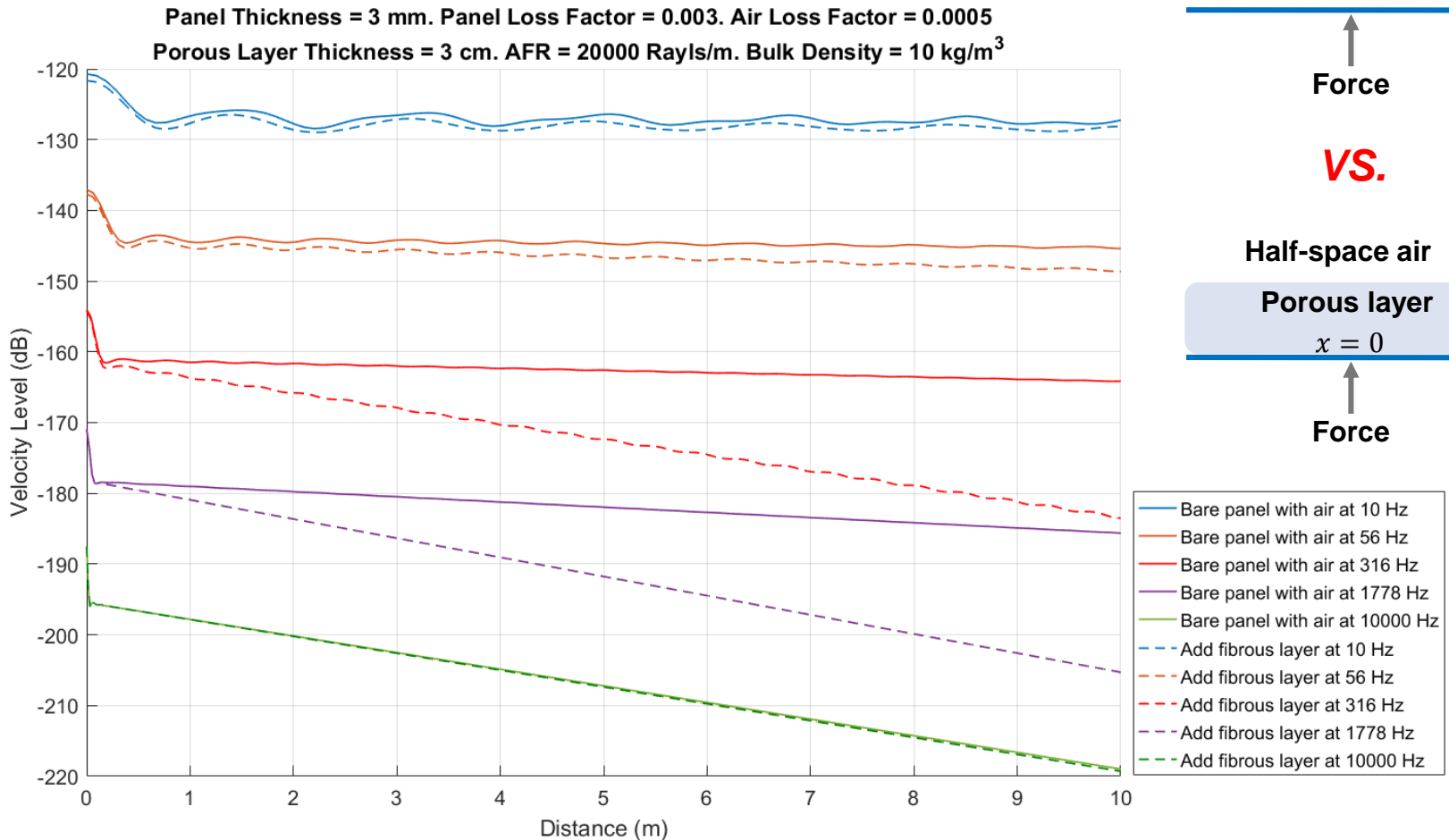


- Fiber Microstructure Design for Optimal Damping Performance



RESULTS - OBSERVATION 1

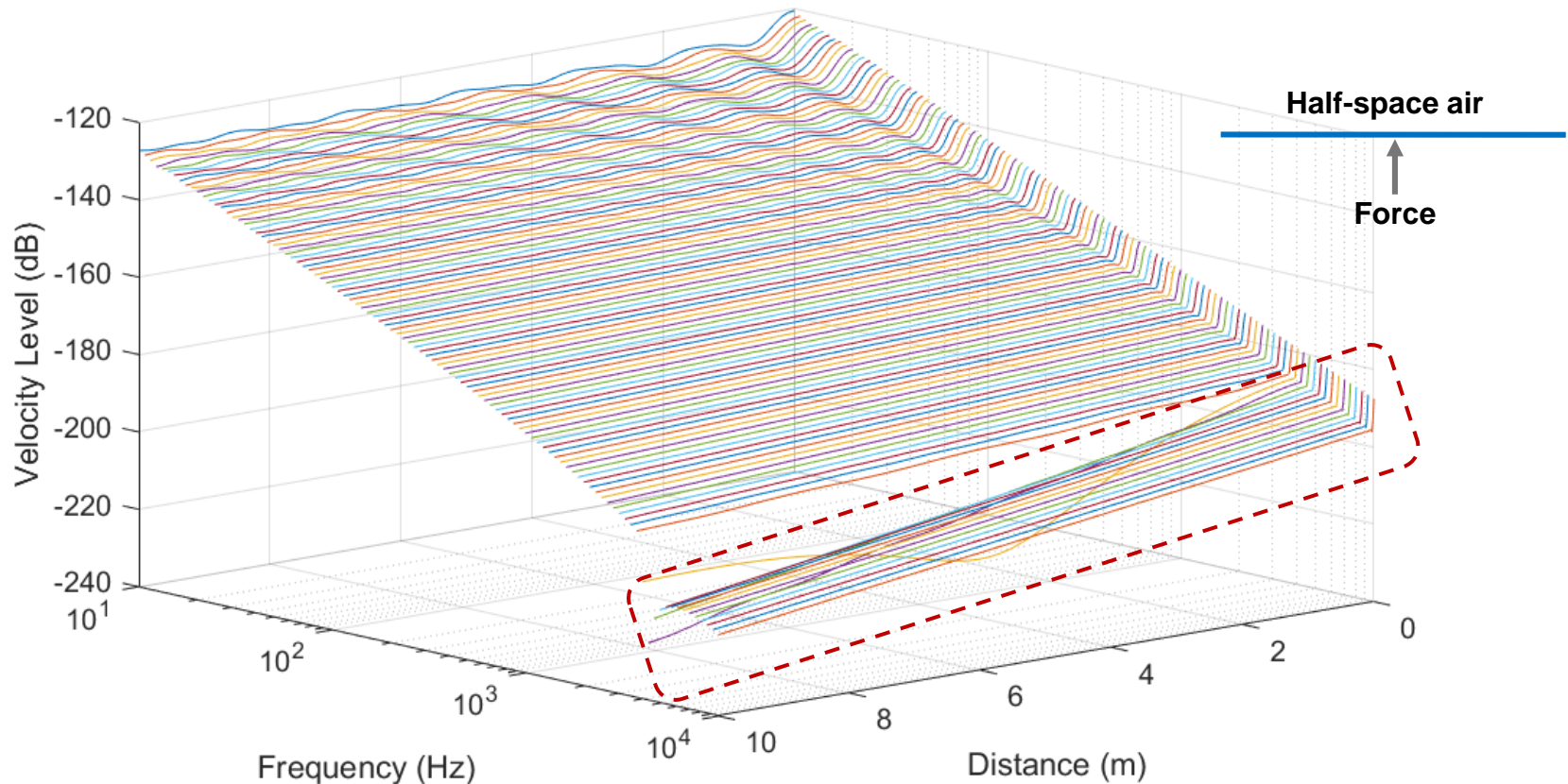
- Spatial Velocity Level (dB)



RESULTS – OBSERVATION 1

- **Spatial Velocity Level (dB)**

Total points $N = 16384$. Wave# sampling rate $\gamma_s = 66\text{-}383\text{rad/m}$. Frequency range = 10-10000Hz
Panel Thickness = 3 mm. Panel Loss Factor = 0.003. Air Loss Factor = 0.0005



- **Spatial resonance in supersonic region above the critical frequency**

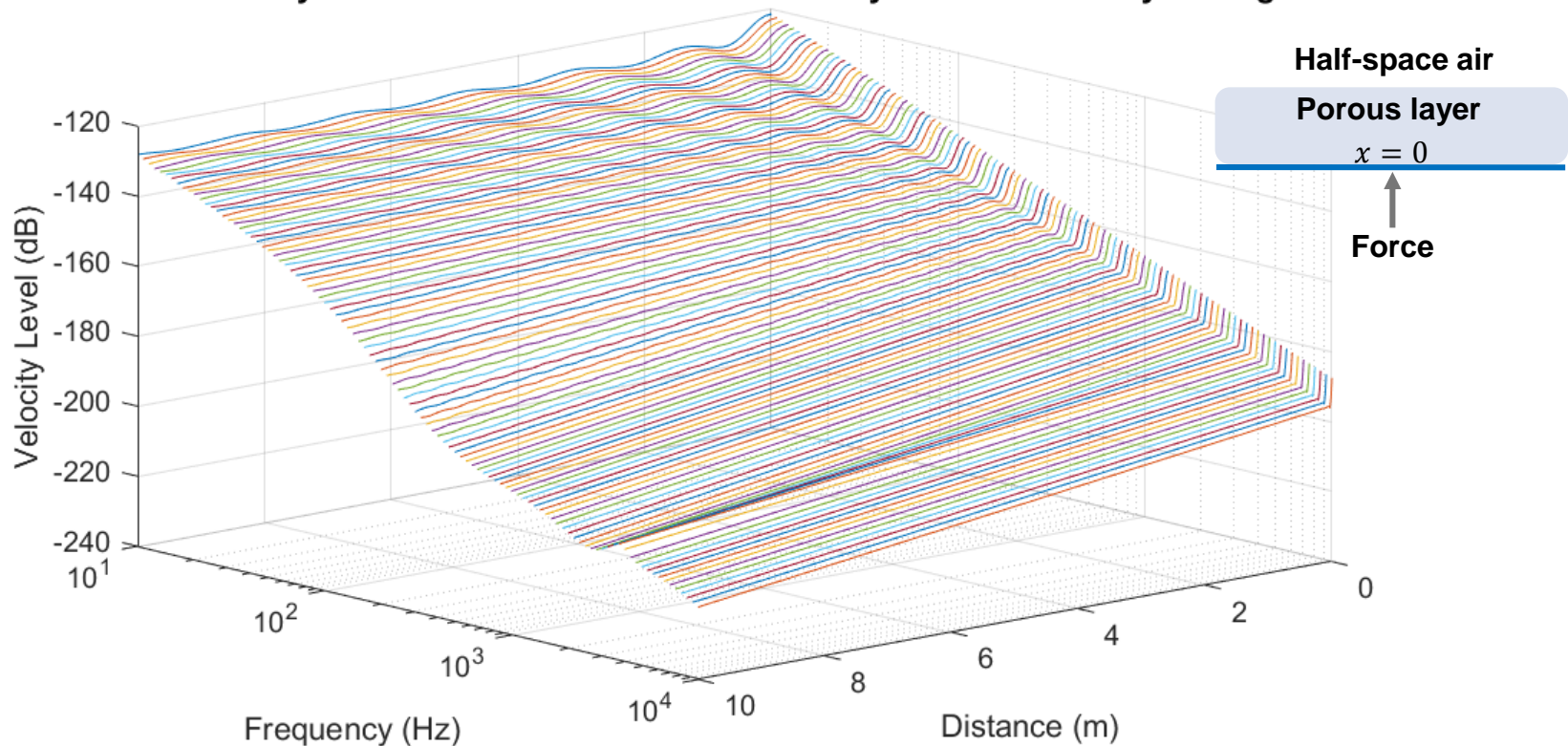
RESULTS – OBSERVATION 1

- Spatial Velocity Level (dB)

Total points $N = 16384$. Wave# sampling rate $\gamma_s = 66\text{-}383$ rad/m. Frequency range = 10-10000 Hz

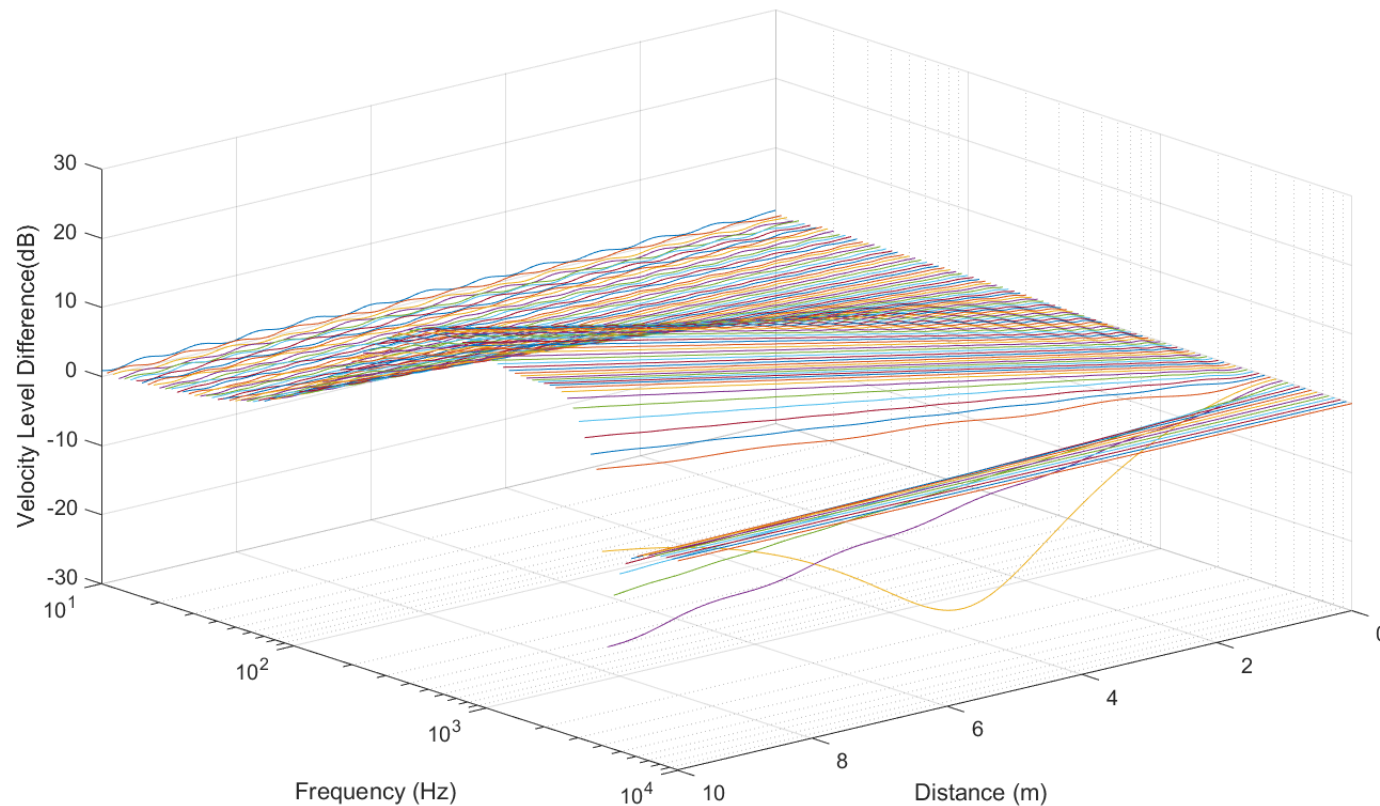
Panel Thickness = 3 mm. Panel Loss Factor = 0.003. Air Loss Factor = 0.0005

Porous Layer Thickness = 3 cm. AFR = 20000 Rayls/m. Bulk Density = 10 kg/m³



RESULTS – OBSERVATION 1

- **Spatial Velocity Level (dB)**
 - **Bare panel case minus Panel + fibers case**

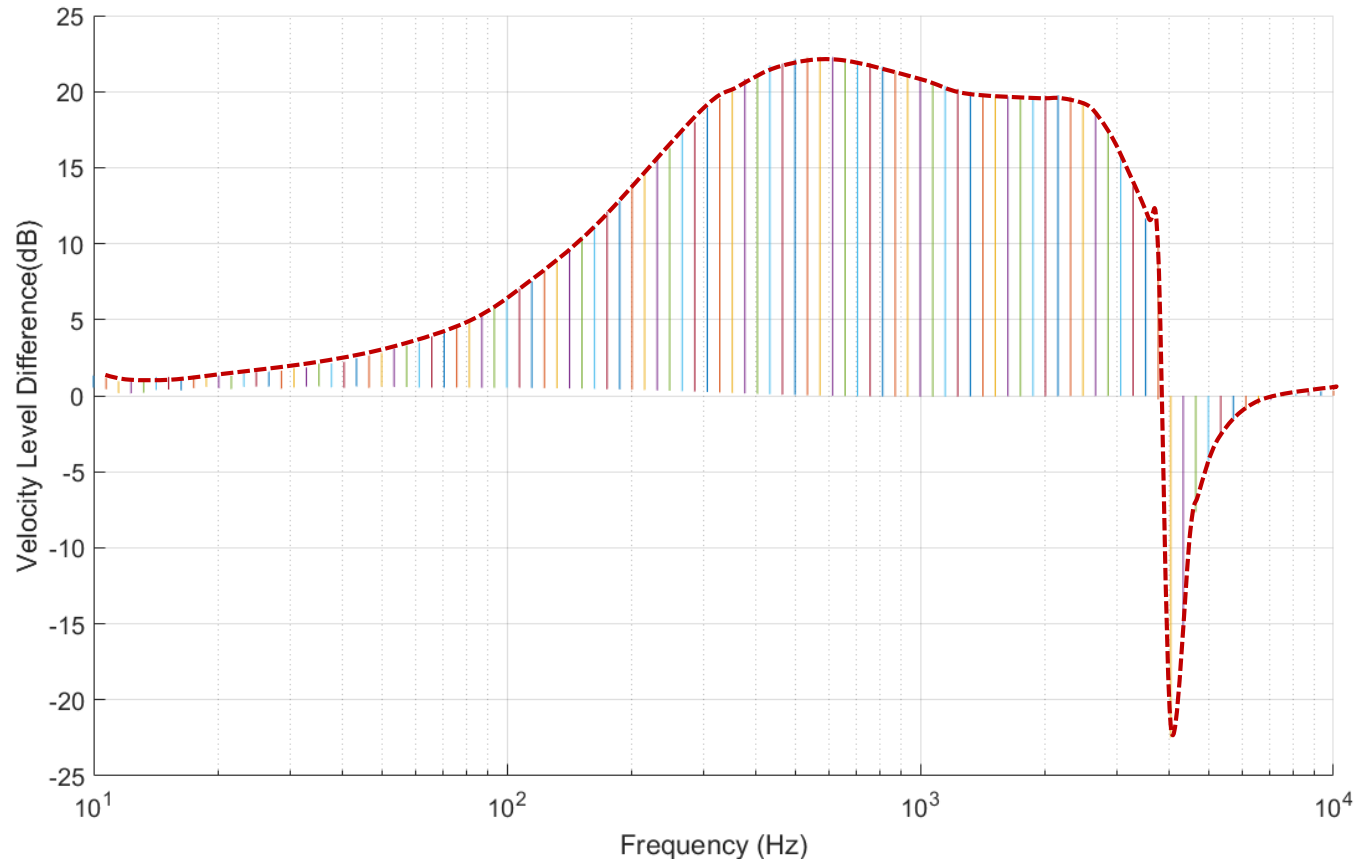


- **Significant attenuation in subsonic region below critical frequency**

RESULTS – OBSERVATION 1

- **Spatial Velocity Level (dB)**

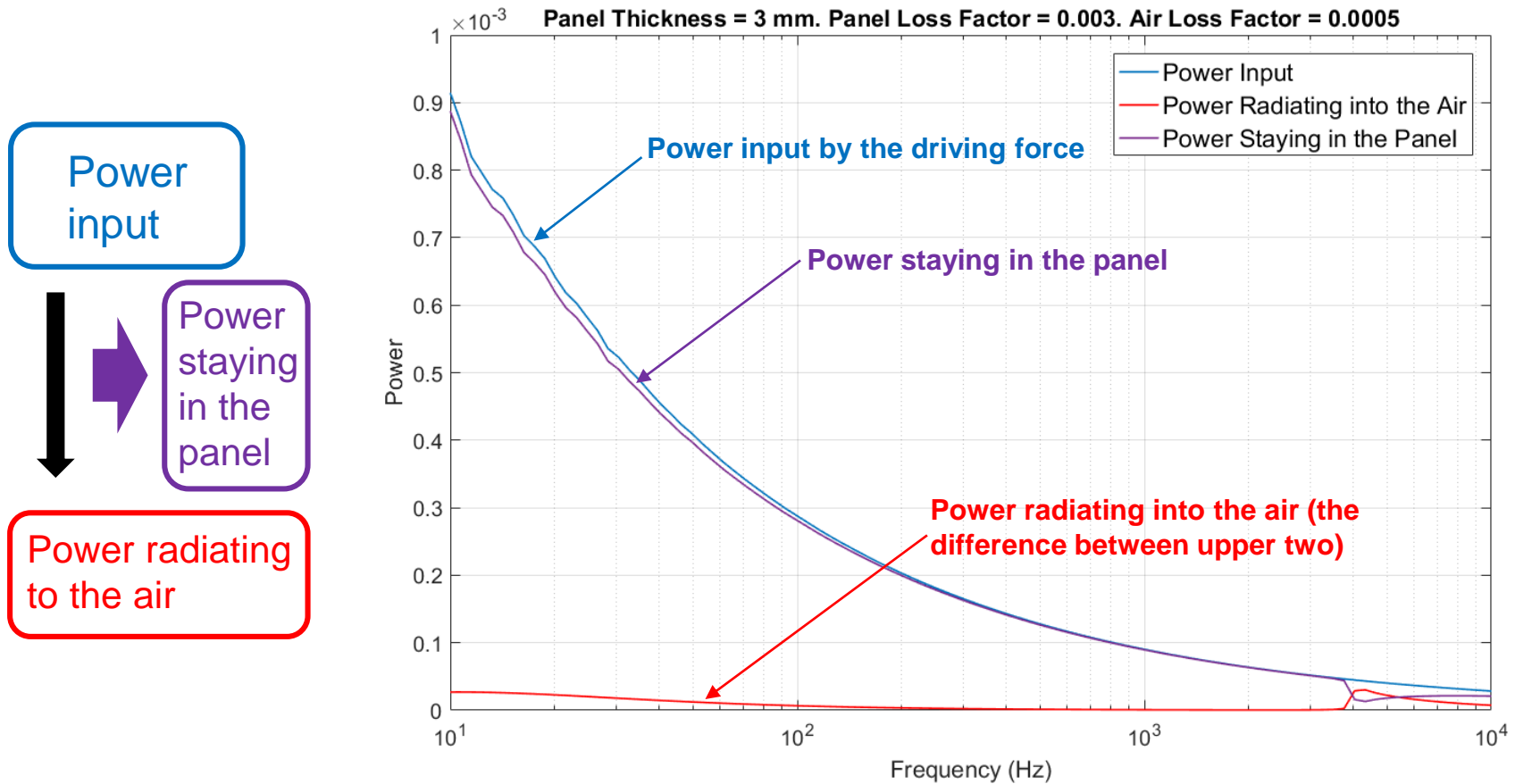
- **Bare panel case minus Panel + fibers case**



- **Significant attenuation in subsonic region below critical frequency**

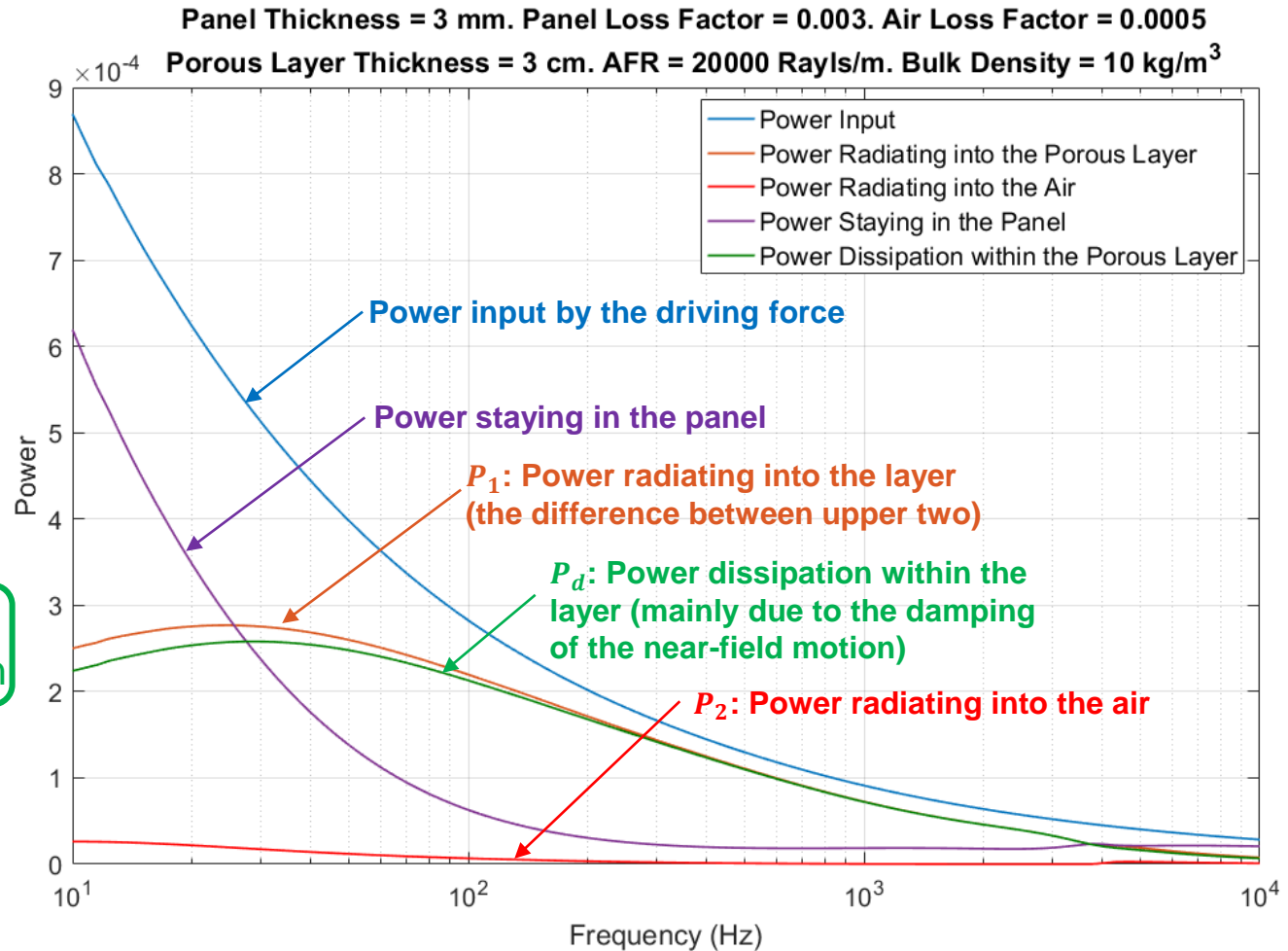
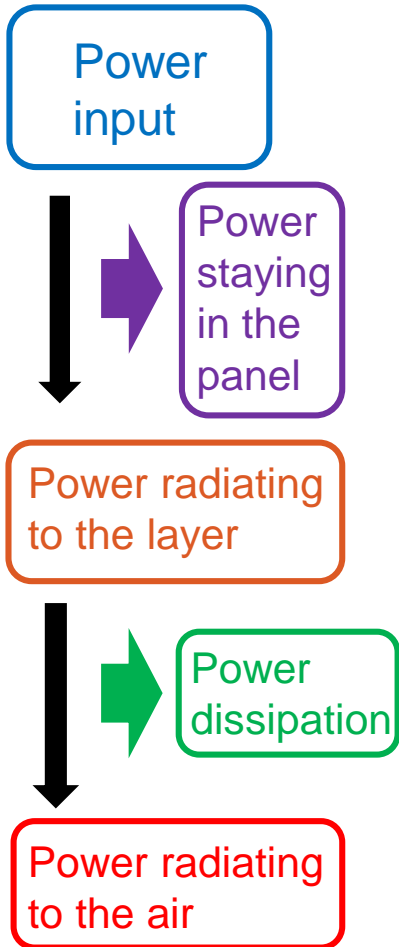
RESULTS – OBSERVATION 2

- Power Distribution – panel + half-space air



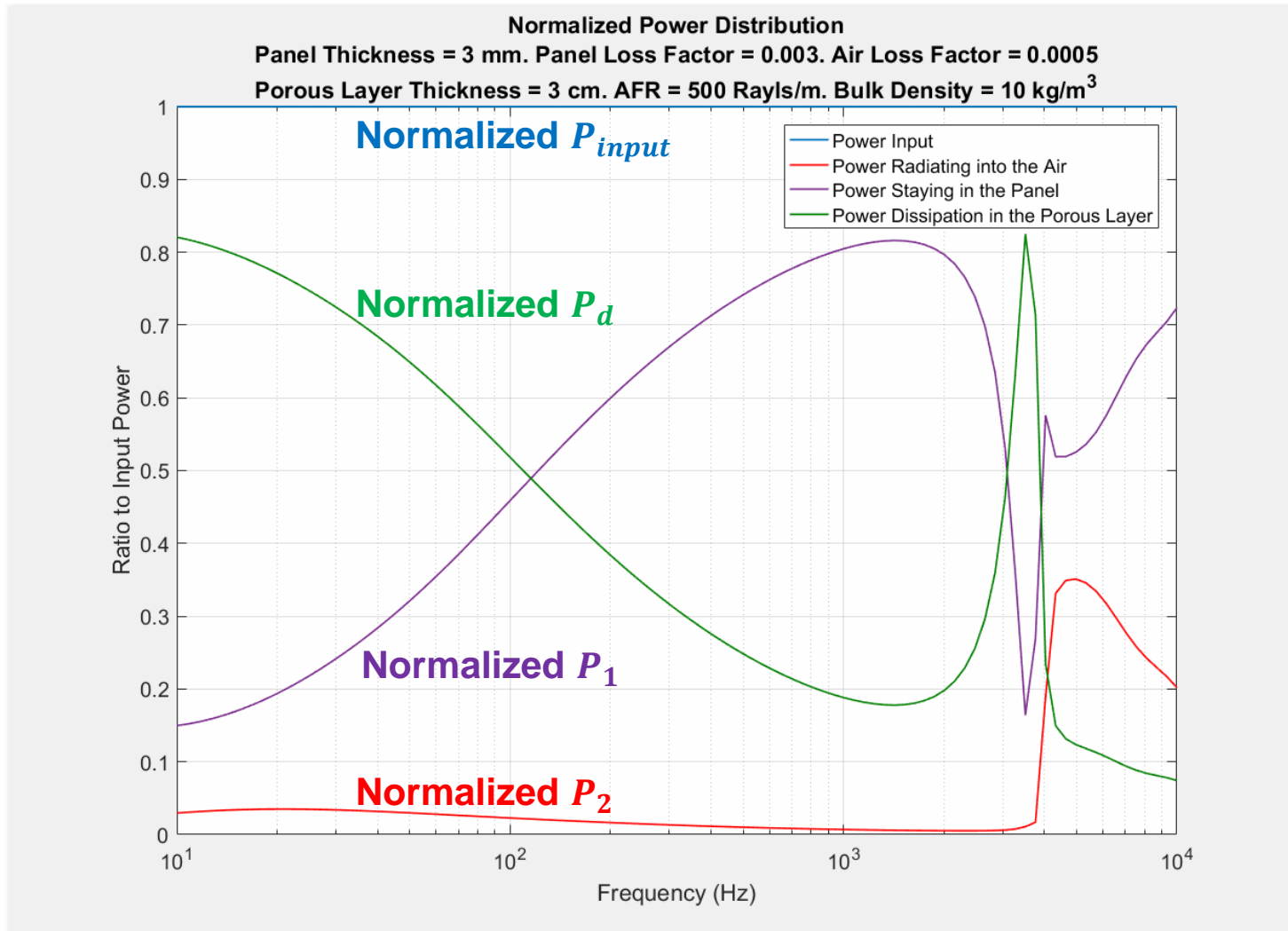
RESULTS – OBSERVATION 2

- Power Distribution – adding limp porous layer



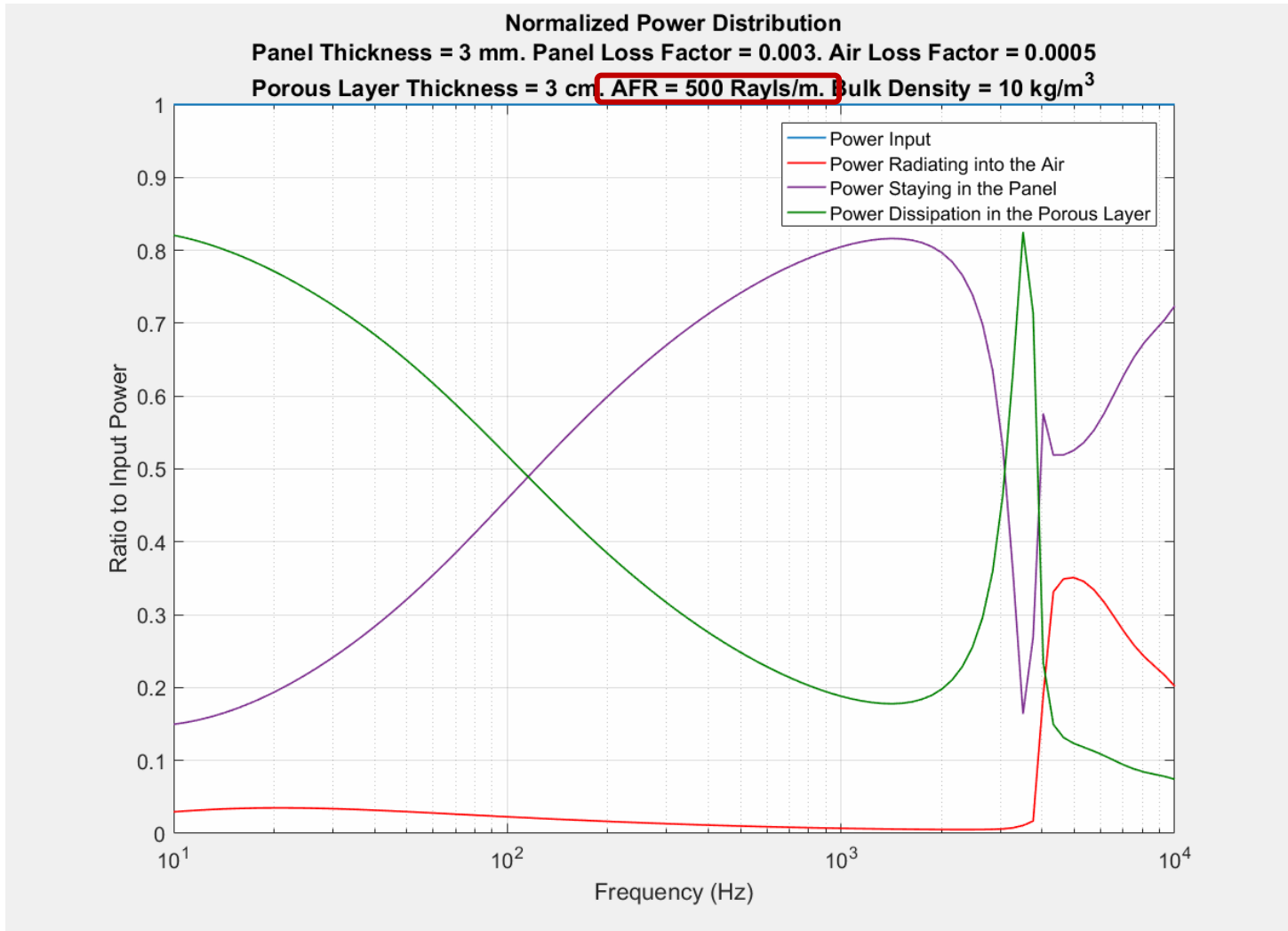
RESULTS - OBSERVATION 3

- Limp Porous Layer Airflow Resistivity Effect on Power Dissipation



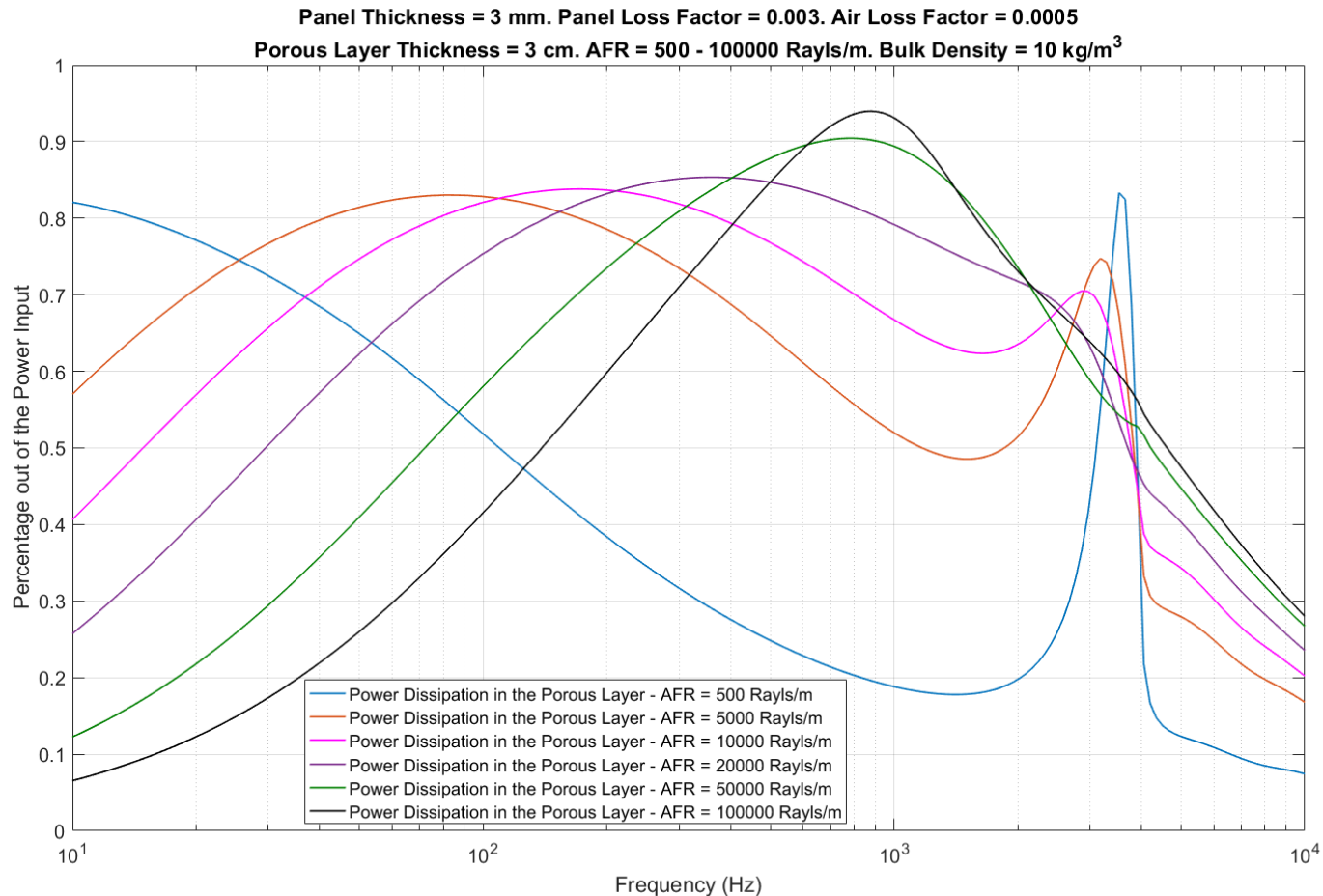
RESULTS - OBSERVATION 3

- Limp Porous Layer Airflow Resistivity Effect on Power Dissipation



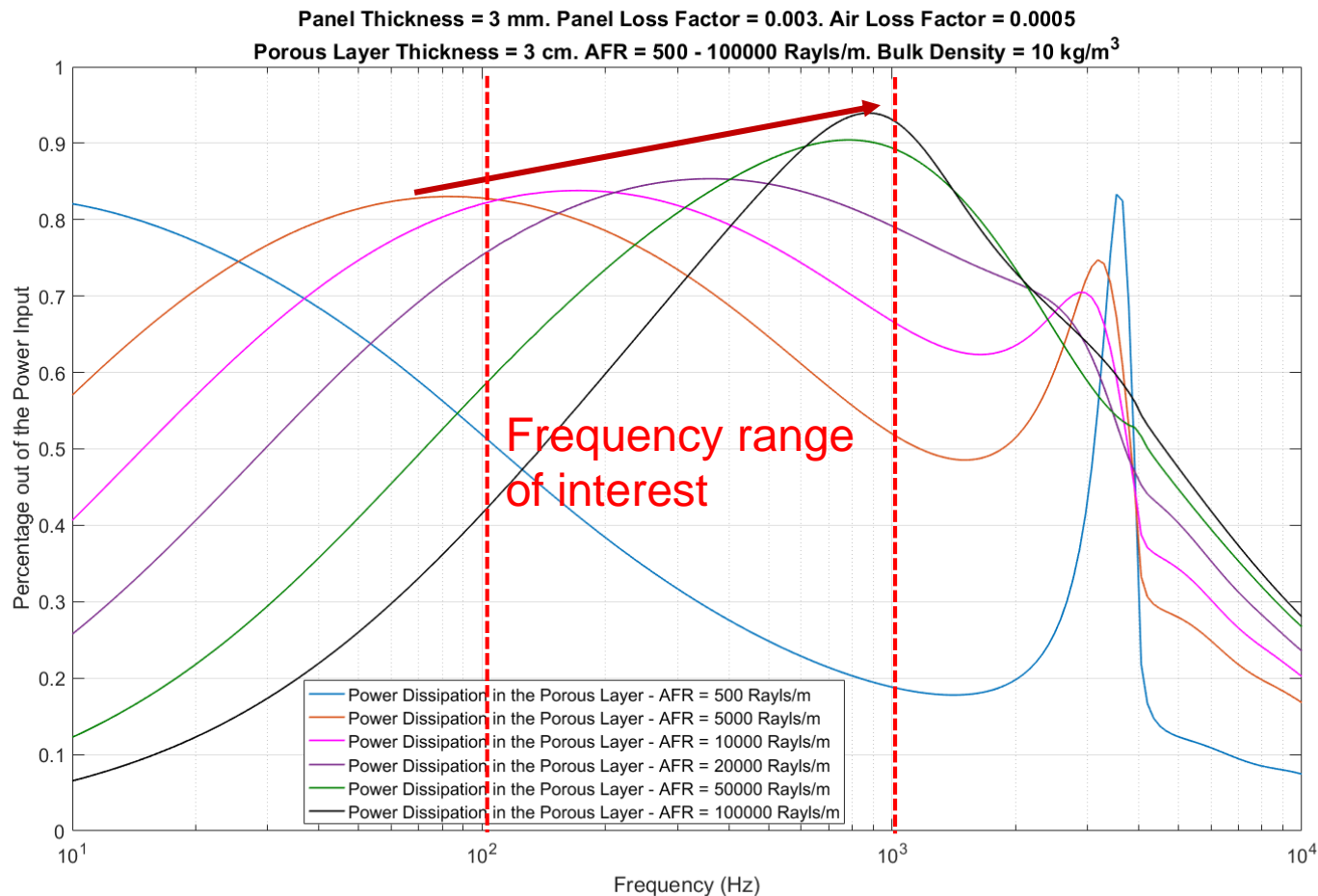
RESULTS - OBSERVATION 3

- Limp Porous Layer Airflow Resistivity Effect on Power Dissipation



RESULTS - OBSERVATION 3

- Limp Porous Layer Airflow Resistivity Effect on Power Dissipation

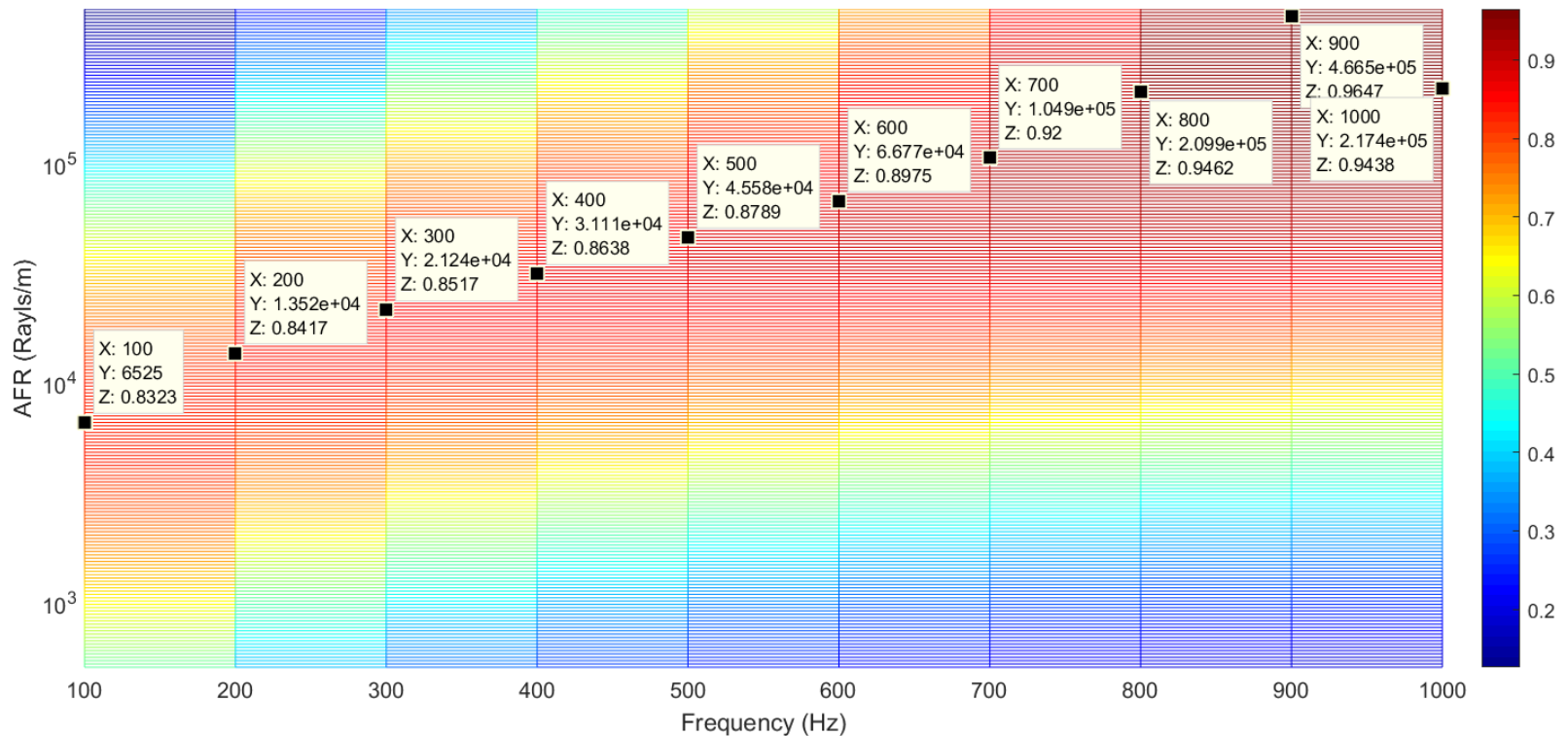


- Optimal damping corresponds to different optimal AFRs at different frequencies

RESULTS – OBSERVATION 3

- **Finding Optimal Fiber Size for Optimal Damping – identifying optimal AFRs**

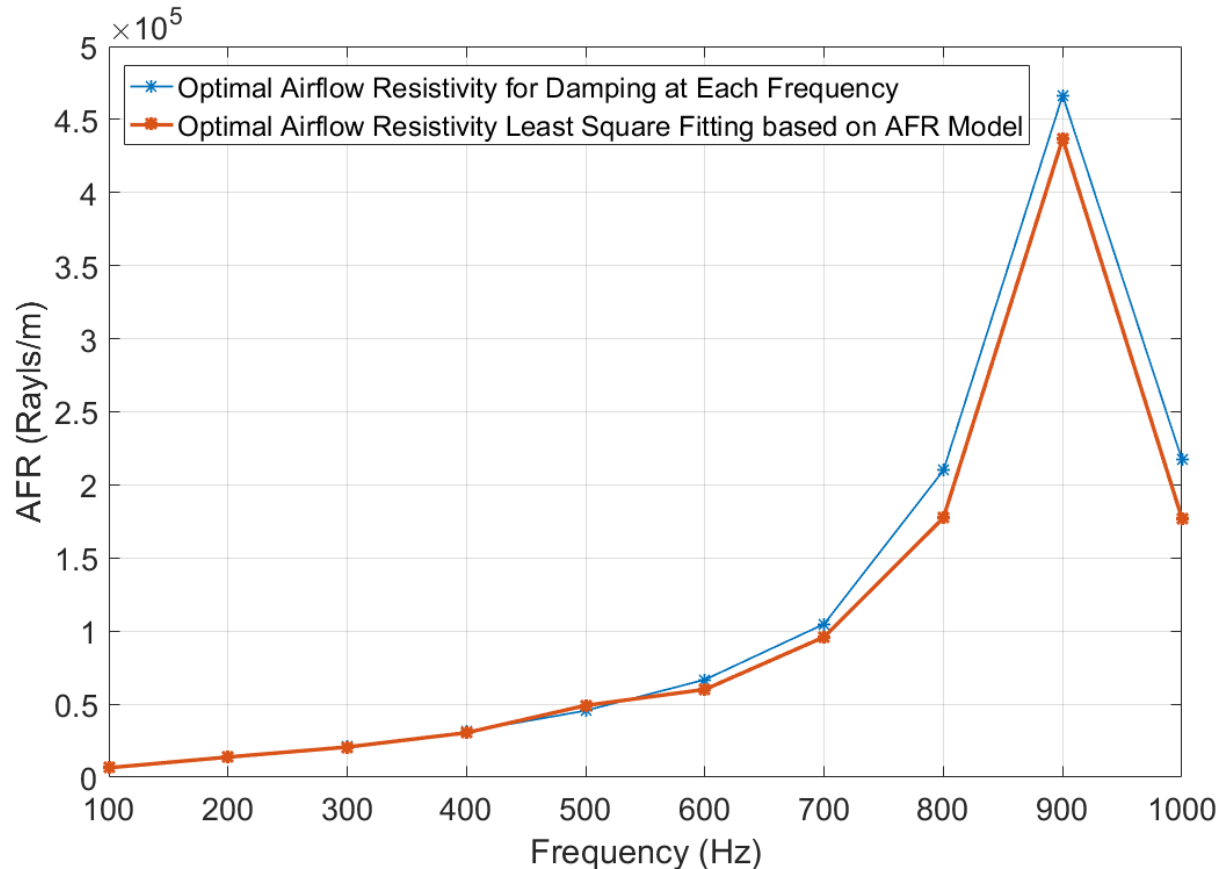
- Aluminum panel thickness = 3 mm; Loss factor = 0.003; Air loss factor = 0.0005
- Polymer fibrous layer thickness = 3 cm; Bulk density = 10 kg/m³; Tortuosity = 1.2; Porosity = 99%



RESULTS – OBSERVATION 4

• Finding Optimal Fiber Size for Optimal Damping – least square fitting AFRs

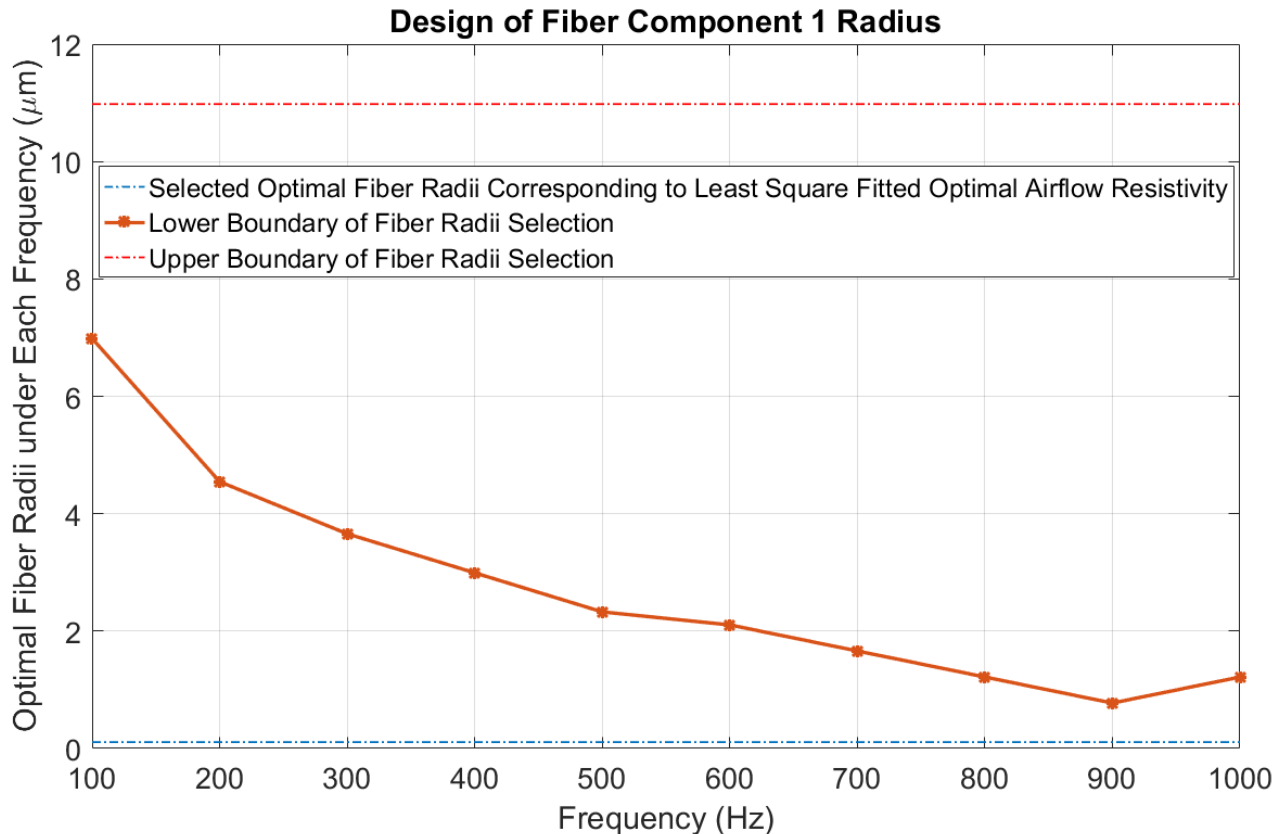
- Aluminum panel thickness = 3 mm; Loss factor = 0.003; Air loss factor = 0.0005
- Polymer fibrous layer thickness = 3 cm; Bulk density = 10 kg/m³; Tortuosity = 1.2; Porosity = 99%
- Fiber inputs: $\rho_1 = 910 \text{ kg/m}^3$; $\rho_2 = 1380 \text{ kg/m}^3$; $X_1 = X_2 = 50\%$; $r_2 = 13 \text{ }\mu\text{m}$; $r_1 \rightarrow$ design target



RESULTS – OBSERVATION 4

• Finding Optimal Fiber Size for Optimal Damping – translating into optimal fiber sizes

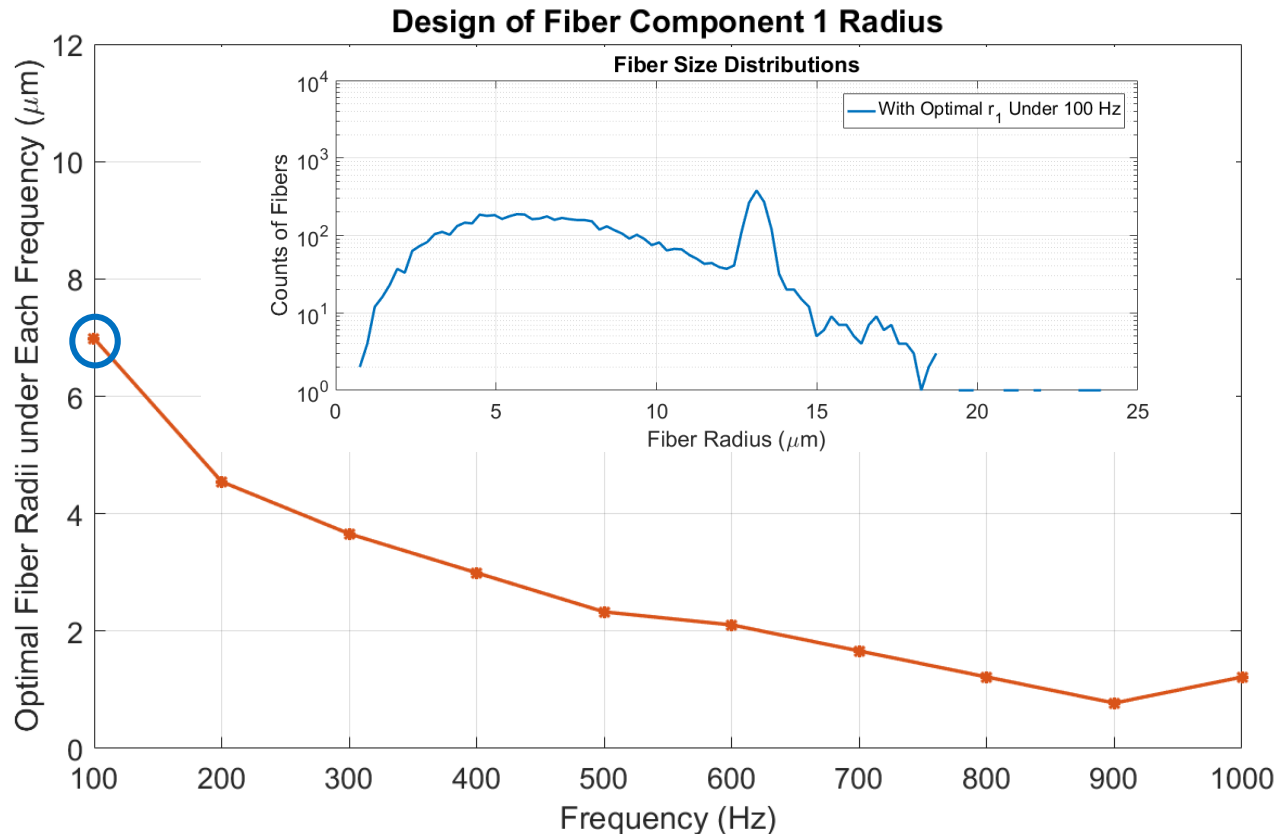
- Aluminum panel thickness = 3 mm; Loss factor = 0.003; Air loss factor = 0.0005
- Polymer fibrous layer thickness = 3 cm; Bulk density = 10 kg/m³; Tortuosity = 1.2; Porosity = 99%
- Fiber inputs: $\rho_1 = 910 \text{ kg/m}^3$; $\rho_2 = 1380 \text{ kg/m}^3$; $X_1 = X_2 = 50\%$; $r_2 = 13 \text{ }\mu\text{m}$; $r_1 \rightarrow$ design target



RESULTS – OBSERVATION 4

• Finding Optimal Fiber Size for Optimal Damping – translating into optimal fiber sizes

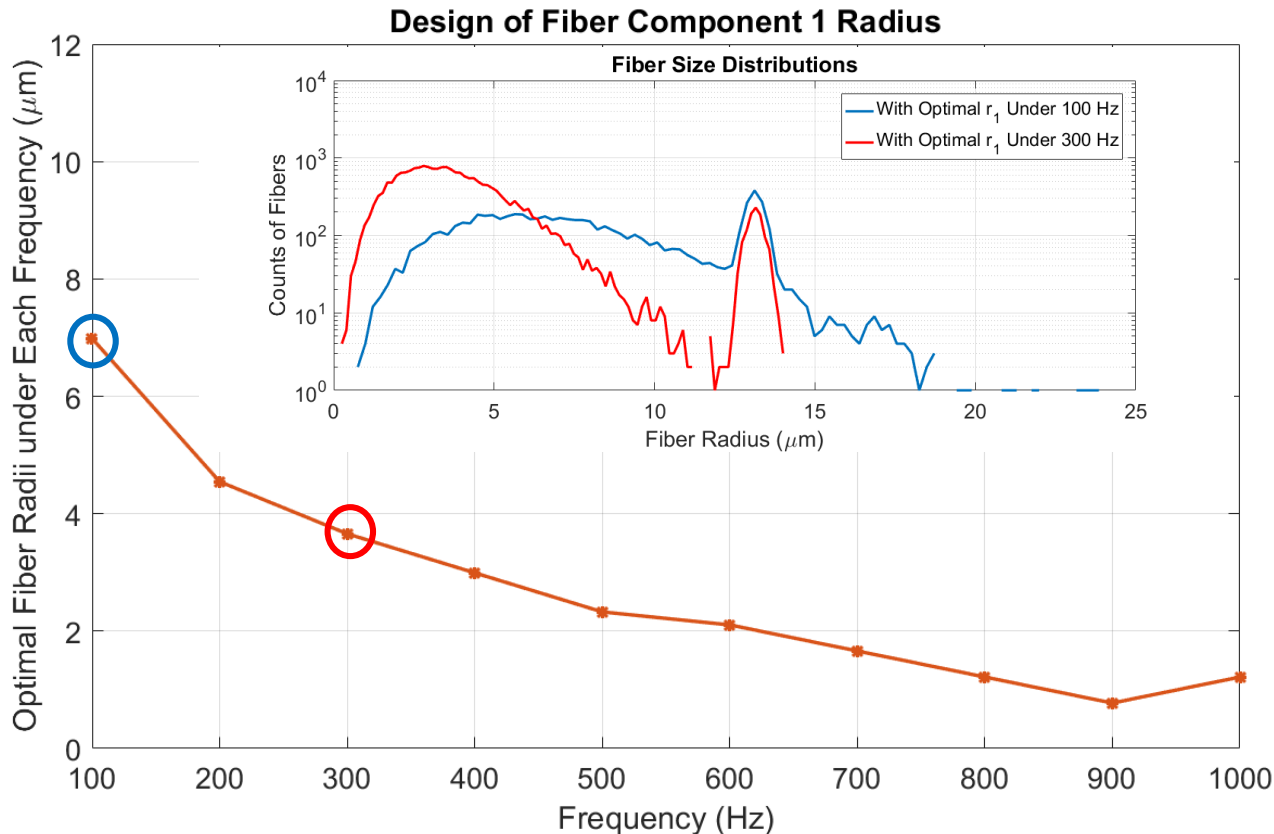
- Aluminum panel thickness = 3 mm; Loss factor = 0.003; Air loss factor = 0.0005
- Polymer fibrous layer thickness = 3 cm; Bulk density = 10 kg/m³; Tortuosity = 1.2; Porosity = 99%
- Fiber inputs: $\rho_1 = 910 \text{ kg/m}^3$; $\rho_2 = 1380 \text{ kg/m}^3$; $X_1 = X_2 = 50\%$; $r_2 = 13 \text{ }\mu\text{m}$; $r_1 \rightarrow$ design target



RESULTS – OBSERVATION 4

• Finding Optimal Fiber Size for Optimal Damping – translating into optimal fiber sizes

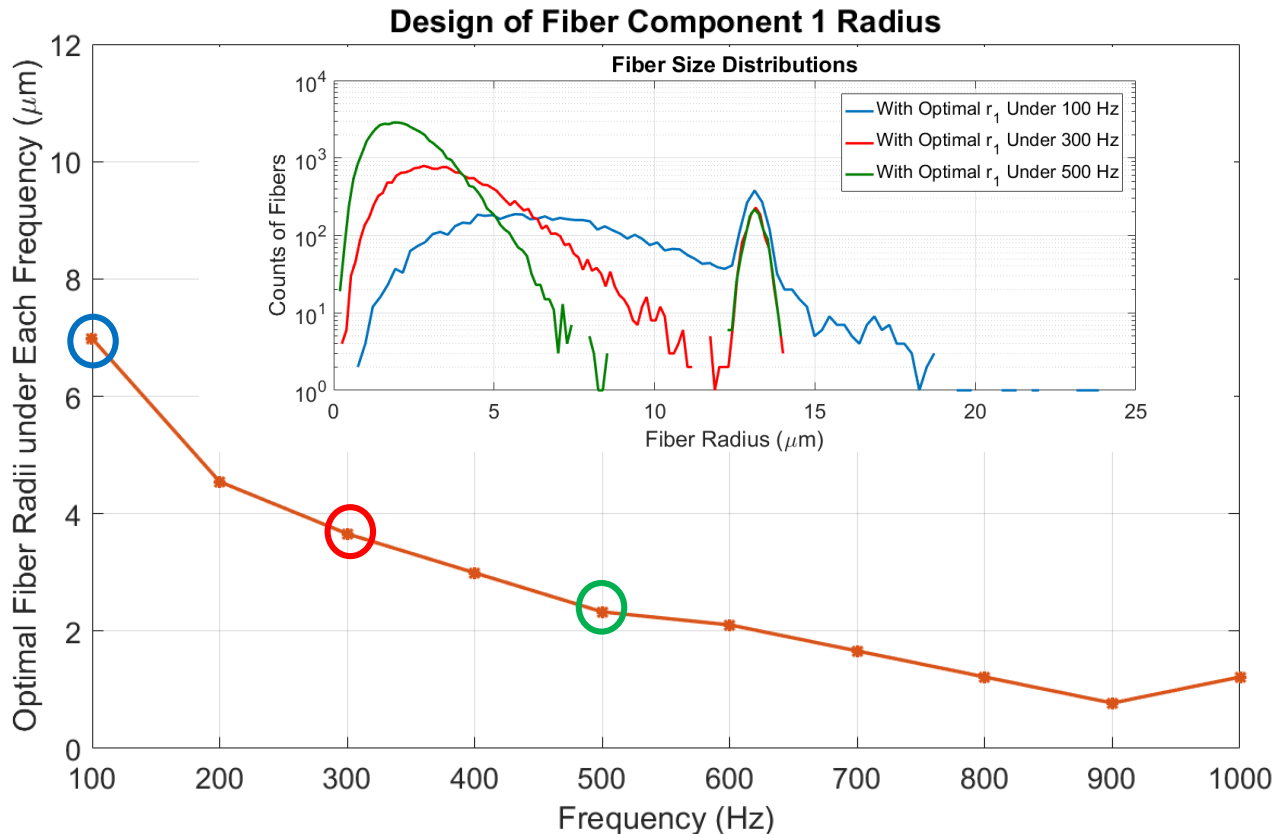
- Aluminum panel thickness = 3 mm; Loss factor = 0.003; Air loss factor = 0.0005
- Polymer fibrous layer thickness = 3 cm; Bulk density = 10 kg/m³; Tortuosity = 1.2; Porosity = 99%
- Fiber inputs: $\rho_1 = 910 \text{ kg/m}^3$; $\rho_2 = 1380 \text{ kg/m}^3$; $X_1 = X_2 = 50\%$; $r_2 = 13 \text{ }\mu\text{m}$; $r_1 \rightarrow$ design target



RESULTS – OBSERVATION 4

• Finding Optimal Fiber Size for Optimal Damping – translating into optimal fiber sizes

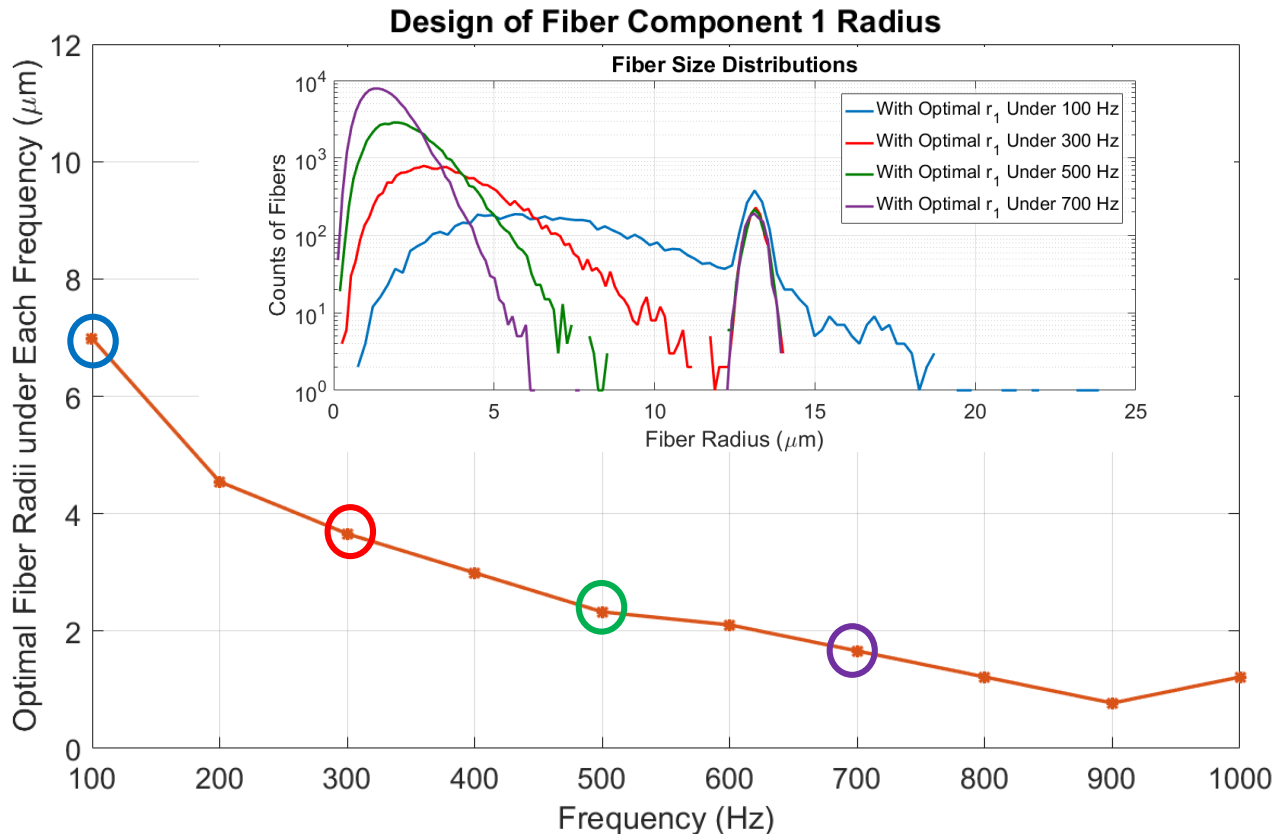
- Aluminum panel thickness = 3 mm; Loss factor = 0.003; Air loss factor = 0.0005
- Polymer fibrous layer thickness = 3 cm; Bulk density = 10 kg/m³; Tortuosity = 1.2; Porosity = 99%
- Fiber inputs: $\rho_1 = 910 \text{ kg/m}^3$; $\rho_2 = 1380 \text{ kg/m}^3$; $X_1 = X_2 = 50\%$; $r_2 = 13 \text{ }\mu\text{m}$; $r_1 \rightarrow$ design target



RESULTS – OBSERVATION 4

• Finding Optimal Fiber Size for Optimal Damping – translating into optimal fiber sizes

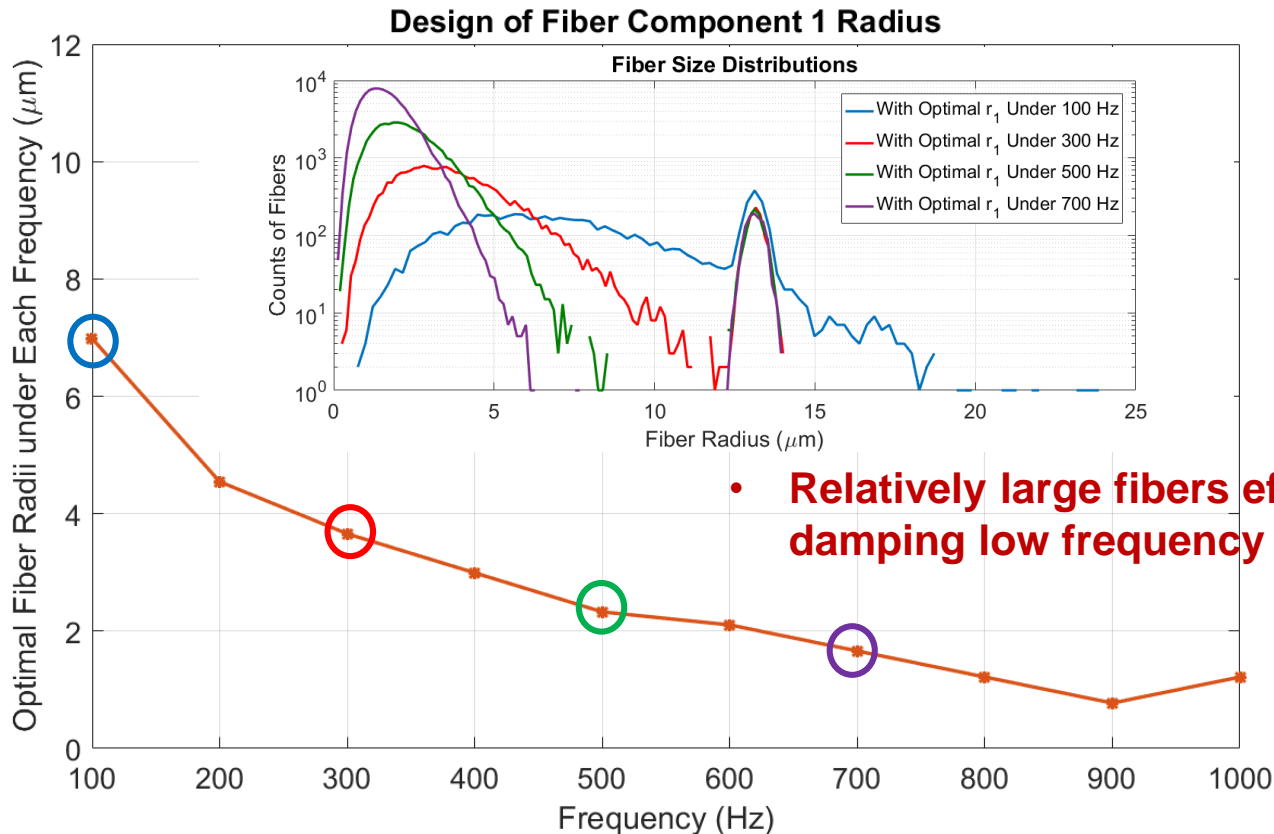
- Aluminum panel thickness = 3 mm; Loss factor = 0.003; Air loss factor = 0.0005
- Polymer fibrous layer thickness = 3 cm; Bulk density = 10 kg/m³; Tortuosity = 1.2; Porosity = 99%
- Fiber inputs: $\rho_1 = 910 \text{ kg/m}^3$; $\rho_2 = 1380 \text{ kg/m}^3$; $X_1 = X_2 = 50\%$; $r_2 = 13 \text{ }\mu\text{m}$; $r_1 \rightarrow$ design target



RESULTS – OBSERVATION 4

• Finding Optimal Fiber Size for Optimal Damping – translating into optimal fiber sizes

- Aluminum panel thickness = 3 mm; Loss factor = 0.003; Air loss factor = 0.0005
- Polymer fibrous layer thickness = 3 cm; Bulk density = 10 kg/m³; Tortuosity = 1.2; Porosity = 99%
- Fiber inputs: $\rho_1 = 910 \text{ kg/m}^3$; $\rho_2 = 1380 \text{ kg/m}^3$; $X_1 = X_2 = 50\%$; $r_2 = 13 \text{ }\mu\text{m}$; $r_1 \rightarrow$ design target

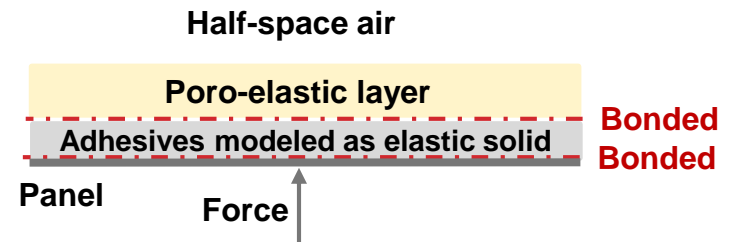
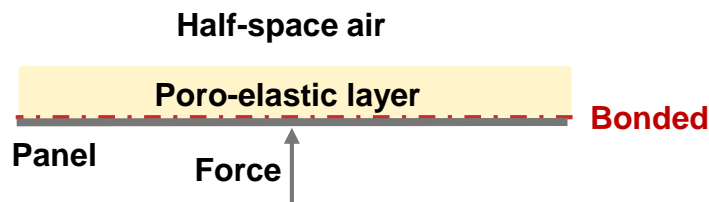
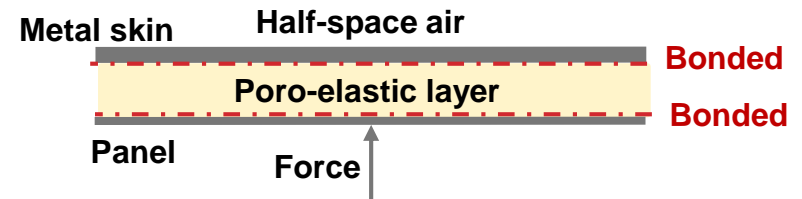
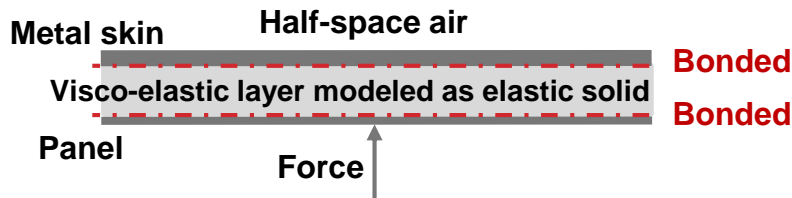
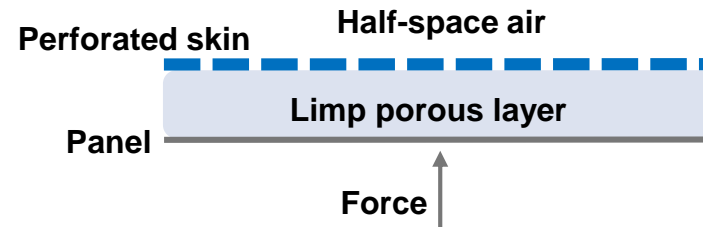
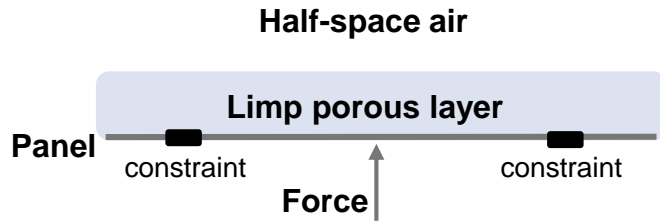


CONCLUSIONS

- Transfer Matrix Method (**TMM**) and Near-field Damping (**NFD**) model based on Inverse Discrete Fourier Transform (IDFT) provide a powerful tool connecting fibrous materials' airflow resistivity with their damping performance
- Modified Airflow Resistivity (**AFR**) model connects fibrous materials' airflow resistivity with their microstructure (*i.e.*, various fiber sizes)
- For a limp porous layer attached to a stiff panel, an optimal airflow resistivity can be found to provide optimal damping performance (**subsonic region power dissipation within the fibrous layer**) under each frequency based on **TMM** and **NFD**
- Corresponding to the optimal airflow resistivity, an optimal fiber size then can be found to provide optimal damping performance under each frequency based on **AFR** and numerical optimization method
- **Relatively large fibers are effective at damping low frequency vibration**

EXTENSION

- Other cases that have been built by the “TMM + NFD + AFR” model



ACKNOWLEDGEMENTS



We sincerely thank 3M for their financial support, and for the technical support from Jonathan Alexander, Myles Brostrom, Ronald Gerdes, Tom Hanschen, Thomas Herdtle, Seungkyu Lee and Taewook Yoo.

REFERENCES



- [1] https://www.3m.com/3M/en_US/company-us/all-3m-products/~/3M-Damping-Aluminum-Foam-Sheets-4014?N=5002385+3293241431&rt=rud
- [2] <http://www.noisedamp.com/>
- [3] <http://multimedia.3m.com/mws/media/1055323O/3m-thinsulate-acoustic-insulation-tc3403-datasheet.pdf>
- [4] R. W. Gerdes, J. H. Alexander, J. S. Bolton, B. K. Gardner and H.-Y. Lai, "Numerical modeling of the damping effect of fibrous acoustical treatments," *Proceedings of the 2001 SAE Noise and Vibration Conference*, (01NVC-71), 7 pages, Traverse City, Michigan, May 2001.
- [5] C. Bruer, J. S. Bolton, "Vibro-Acoustic Damping of Extended Vibrating Systems," *11th Aeroacoustics Conference*, AIAA-87-2661, 7 pages, Palo Alto, California, October 1987.
- [6] T. J. Wahl and J. S. Bolton, "The Use of the Discrete Fourier Transform to Calculate the Spatial and Temporal Response of Line-Driven, Layer-wise Homogeneous Acoustically Loaded Panels," *Journal of the Acoustical Society of America*, Vol. 92, pp. 1473-1488, 1992 .
- [7] H.-Y. Lai, J. S. Bolton, "Structural Damping by the Use of Fibrous Blankets," *Proceedings of the 1998 Noise and Vibration Conference*, Session 47.3 Vibration and Shack, pp. 403-408, Ypsilanti, Michigan, April 1998.
- [8] R. W. Gerdes, J. H. Alexander, J. S. Bolton, B. K. Gardner and H.Y. Lai, "The Use of Poro-elastic Finite Elements to Model the Structural Damping effect of Fibrous Acoustical Treatments," *Proceedings of the 1998 Noise Conference*, Session 47.3 Vibration and Shack, pp. 409-414, Ypsilanti, Michigan, April 1998.
- [9] S. Nadeau, Y. Champoux and L. Mongeau, "Trim and Floor Influence on Vibrational Response of an Aircraft Model," *Journal of Aircraft*, Vol. 36, No. 3, pp. 591-595, May-June 1999
- [10] Yutong Xue, J. S. Bolton, Ronald Gerdes, Seungkyu Lee and Thomas Herdtle, "Prediction of airflow resistivity of fibrous acoustical media having double fiber components and a distribution of fiber radii," *Proceedings of Inter-Noise 2017*, pp. 5649-5657, Hong Kong, August 2017.